PERGAMON

Journal of Structural Geology 25 (2003) 793–812

JOURNAL OF STRUCTURAL GEOLOGY

www.elsevier.com/locate/jsg

Mesoscale strike-slip faults and damage zones at Marsalforn, Gozo Island, Malta

Young-Seog Kim[a,1], D.C.P. Peacock[b,*], David J. Sanderson[c]

[a]*School of Ocean and Earth Science, University of Southampton, Southampton SO14 3ZH, UK*
[b]*Robertson Research International Ltd, Llandudno LL30 1SA, UK*
[c]*Department of Earth Science and Engineering, Imperial College, London SW7 2BP, UK*

Received 20 December 2000; received in revised form 12 December 2001; accepted 4 December 2002

Abstract

Well-exposed strike-slip faults in limestones in the north-western part of Gozo show damage zones that can be grouped into three categories based on their location along faults; tip damage, linking damage and distributed damage. The predominant fracture types within damage zones include extension fractures and secondary faults. Tip damage zones usually show wedge-shaped patterns formed by antithetic faults and extension fractures, commonly accompanied by block rotation. Several fractures are combined at linking damage zones, typically with the concentration of a high intensity of fractures. Structures in distributed damage zones are typically similar to the classical Riedel shear pattern. Evolutionary and 3D models are proposed in terms of the geometries of damage zones for small displacement strike-slip fault zones. Different evolutionary routes depend on fault tip modes and locations.

Keywords: Strike-slip faults; Damage zones; Fracture types

1. Introduction

Secondary faults and extension fractures are heterogeneously developed in fault zones and can play a critical role in fault growth (e.g. Cowie and Scholz, 1992; McGrath and Davison, 1995). Small and meso-scale faults are not generally planar surfaces, but are commonly zones of linked en échelon fractures (e.g. Gamond 1987) at a variety of scales (e.g. Tchalenko, 1970). Fluid flow along faults may also be heterogeneous and channelled within regions of highly fractured rock (e.g. Caine et al., 1996; Sibson, 1996; Dholakia et al., 1998; Martel and Boger, 1998).

1.1. Terminology

Any type of fracturing that is spatially associated with a fault zone will be referred to in this study as *damage*. Damage zones around faults can occur because of stress concentrations, particularly at fault tips and linkage zones (e.g. Chester and Logan, 1986; Wu and Groshong, 1991; Cowie and Scholz, 1992; Peacock and Sanderson, 1995a; Gupta and Scholz, 2000) or to accommodate displacement variations along faults (Kim et al., 2000). Damage can thus provide important information on the propagation, evolution and termination of a fault zone.

Fault is used here where a measurable displacement can be observed or confidently inferred. The sense of displacement on secondary faults is inferred from offset of fossils or earlier fractures, from pull-apart geometries, and from *wing cracks* (e.g. Willemse and Pollard, 1998). The *master* faults are the longest and widest faults, and have the largest displacements. *Extension fractures* have opening normal to the fracture walls, and include joints and some veins. The term *fracture* is used as a general term for faults and extension fractures, for example when the sense of displacement is not known. The along-strike tips of strike-slip faults are mode II (shear parallel to the plane of the fracture and perpendicular to the crack edge) fault tips, while up- and down-dip tips are mode III (shear parallel to the plane of the fracture and parallel to the crack edge) tips (Atkinson, 1987; Pollard and Segall, 1987; McGrath and

* Corresponding author. Tel.: +44-1492-581811; fax: +44-1492-583416.
E-mail address: dcp@robresint.co.uk (D.C.P. Peacock).
[1] Now at: School of Earth and Environmental Sciences, Seoul National University, Seoul 151-747, Korea.

0191-8141/03/$ - see front matter © 2003 Elsevier Science Ltd. All rights reserved.
PII: S0191-8141(02)00200-6

Davison, 1995; Martel and Boger, 1998). The term *linkage* is used here to describe understepping or overstepping faults that show evidence of interaction, e.g. connecting fractures between the faults.

Based on analysis of fault zones at Marsalforn and elsewhere, we recognise three types of spatial association between fault traces and damage, which are deliberately non-genetic. (1) *Tip damage* occurs at or ahead of the tip of a fault trace. (2) *Linking damage* occurs in and around the region between fault segments, usually in oversteps between faults. (3) *Distributed damage* occurs along the trace of a fault zone; it is not obviously confined to exposed tips or linkage zones, although this type of damage may be related to such features that do not intersect the exposure surface.

1.2. Previous work on damage zones and the aims of this paper

Relatively little work has been published that uses detailed field investigations to determine how damage zones develop and how they relate to fault propagation. Some field studies have focused on damage zones at the tips of strike-slip (e.g. Rispoli, 1981; Segall and Pollard, 1983; Granier, 1985; Martel et al., 1988; Willemse et al., 1997) or normal (e.g. Cowie and Shipton, 1998) faults. Peacock and Sanderson (1995a) described damage developed in oversteps between strike-slip fault segments. Vermilye and Scholz (1999) present microstructural evidence for the propagation of mesoscale strike-slip faults. McGrath and Davison (1995) and Martel and Boger (1998) published 3D interpretations of fault damage zones.

Fracture development associated with fault growth has also been studied in experiments (e.g. Brace and Bombolakis, 1963; Tchalenko, 1970; Gamond, 1983; Horii and Nemat-Nasser, 1985; Cox and Scholz, 1988; Petit and Barquins, 1988). In addition, theoretical studies have explored the processes of stress concentration and rupture in rock (e.g. Segall and Pollard, 1983; Pollard and Segall, 1987; Scholz, 1990; Reches and Lockner, 1994). These studies have shown that secondary faults and extension fractures commonly initiate oblique to a fault, at locations where the tensile stresses are highest (e.g. Martel and Boger, 1998). These fractures can link originally discontinuous faults both mechanically (Segall and Pollard, 1983; Martel, 1990; Bürgmann et al., 1994; Martel, 1997; Crider and Pollard, 1998) and hydraulically (Long and Witherspoon, 1985; National Academy of Science, 1996). As a result, secondary faults and extension fractures greatly influence how faults grow and how fluids circulate in the Earth's crust (Martel and Boger, 1998; Caine and Forster, 1999).

This paper presents detailed maps of excellently exposed faults at Gozo Island, and these maps are used to develop a 3D model for the damage associated with strike-slip faults. It is the aim of this paper to use the mapped distribution together with information on the type, orientation, and opening/slip sense of faults and extension fractures to infer the relationships of damage to faulting.

1.3. Geological setting

This paper describes the geometry of damage zones around well-exposed strike-slip faults in limestone at Marsalforn (latitude 36°5′N, longitude 14°11′E), Gozo Island, Malta. The 1 km long section between Reqqa Point and Xwieni Bay (Fig. 1) was selected for study because there is excellent exposure of meso-scale strike-slip faults. The damage zones are from several millimetres to several tens of metres long, and from <10 mm to several metres wide. The faults occur in the Miocene age Lower Globigerina Limestone, which is 5–40 m thick on Gozo (Fig. 1c; Pedley et al., 1976; Debono and Xerri, 1993). It is a pale cream to yellow, massively bedded packstone, rich in planktonic foraminifera, becoming wackestone a short distance above the base. A ubiquitous hard ground marks the top of the limestone (Pedley et al., 1976; Debono and Xerri, 1993). Stratigraphic evidence suggests deformation at depths of no greater than 1 km (Peacock, 2001).

The island of Gozo is characterised by a flat-lying Oligo–Miocene succession of carbonates with a gentle regional dip to the NE. Major ENE–WSW striking normal faults predominate across most of Malta and Gozo. Fresh fault-scarp faces with striae, negligible scarp recession, and the development of local raised beaches suggest that the faulting must be, in part, recent (Pedley et al., 1976). In the north-western part of Gozo, the normal faults are replaced locally by strike-slip faults (Fig. 2) that are also related to NNW–SSE extension. Peacock (2001, fig. 1) suggests that many of these faults are joints that were reactivated as strike-slip faults as the stress system rotated.

1.4. Research methods

Several well-exposed strike-slip faults and their associated damage zones (Fig. 2), exposed on limestone bedding planes, have been mapped (locations shown on Fig. 1c). Maps of the faults were made from field photographs. The maps were adjusted using field measurements to reduce distortion on the photographs. Displacement senses and magnitudes have been measured wherever possible, e.g. using displaced earlier fractures and the widths of pull-aparts. Damage zones are viewed in terms of their positions in relation to master faults.

2. Orientations and displacements of faults and extension fractures

One hundred and twenty-two faults and extension fractures longer than 1 m can be grouped into three sets (Fig. 3a): right-lateral faults ($n = 21$), left-lateral faults ($n = 39$) and extension fractures ($n = 62$). All faults and

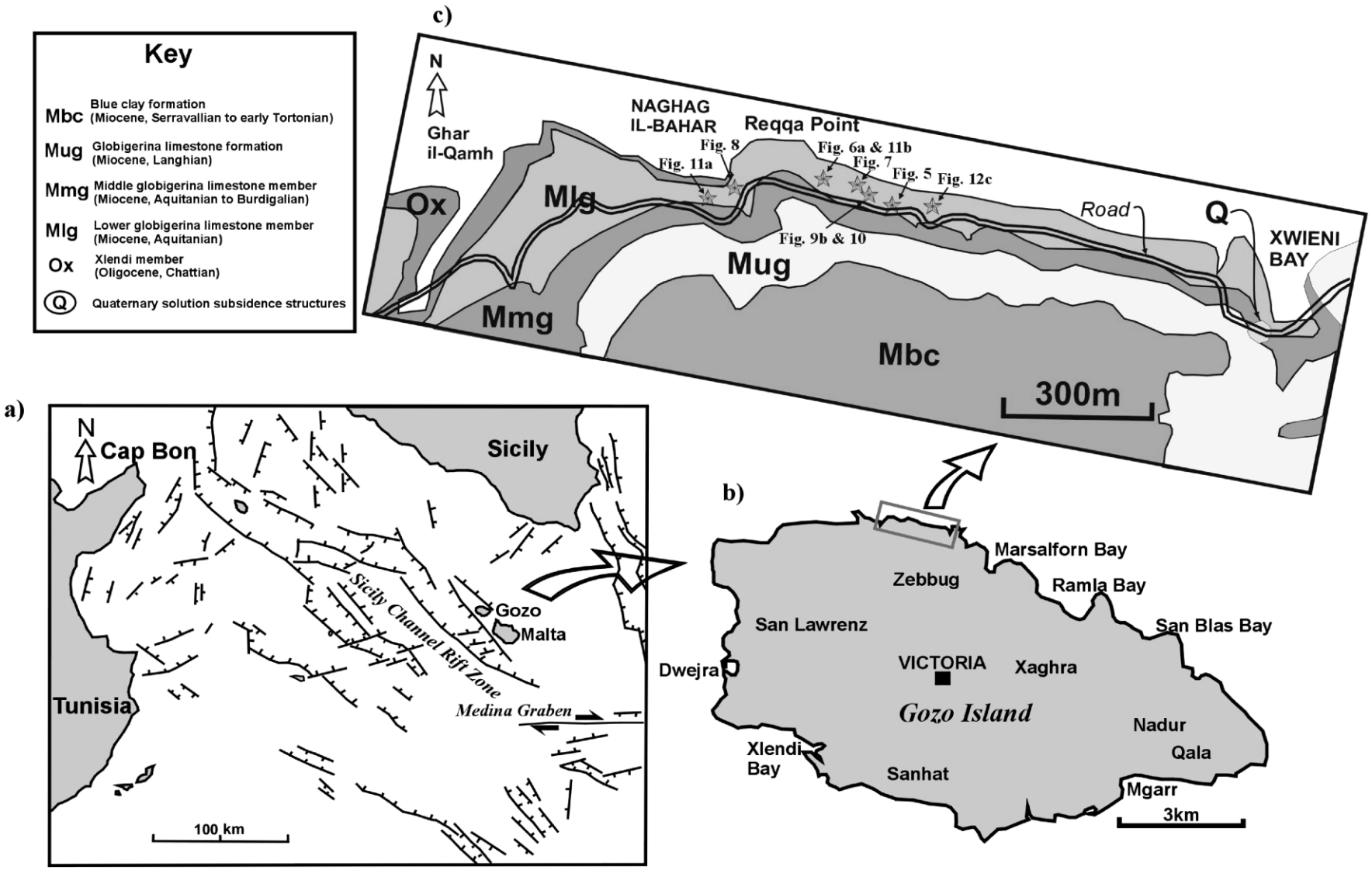

Fig. 1. (a) Sketch map of the Sicily Channel Zone and the Pelagian Block (modified from Finetti, 1984; Boccaletti et al., 1987). (b) Map of Gozo Island showing the location of the study area. (c) The study area, west of Marsalforn, between Reqqa Point and Xwieni Bay. The host rock is the Lower Globigerina Limestone Member (Miocene). Some of the mapped locations are denoted.

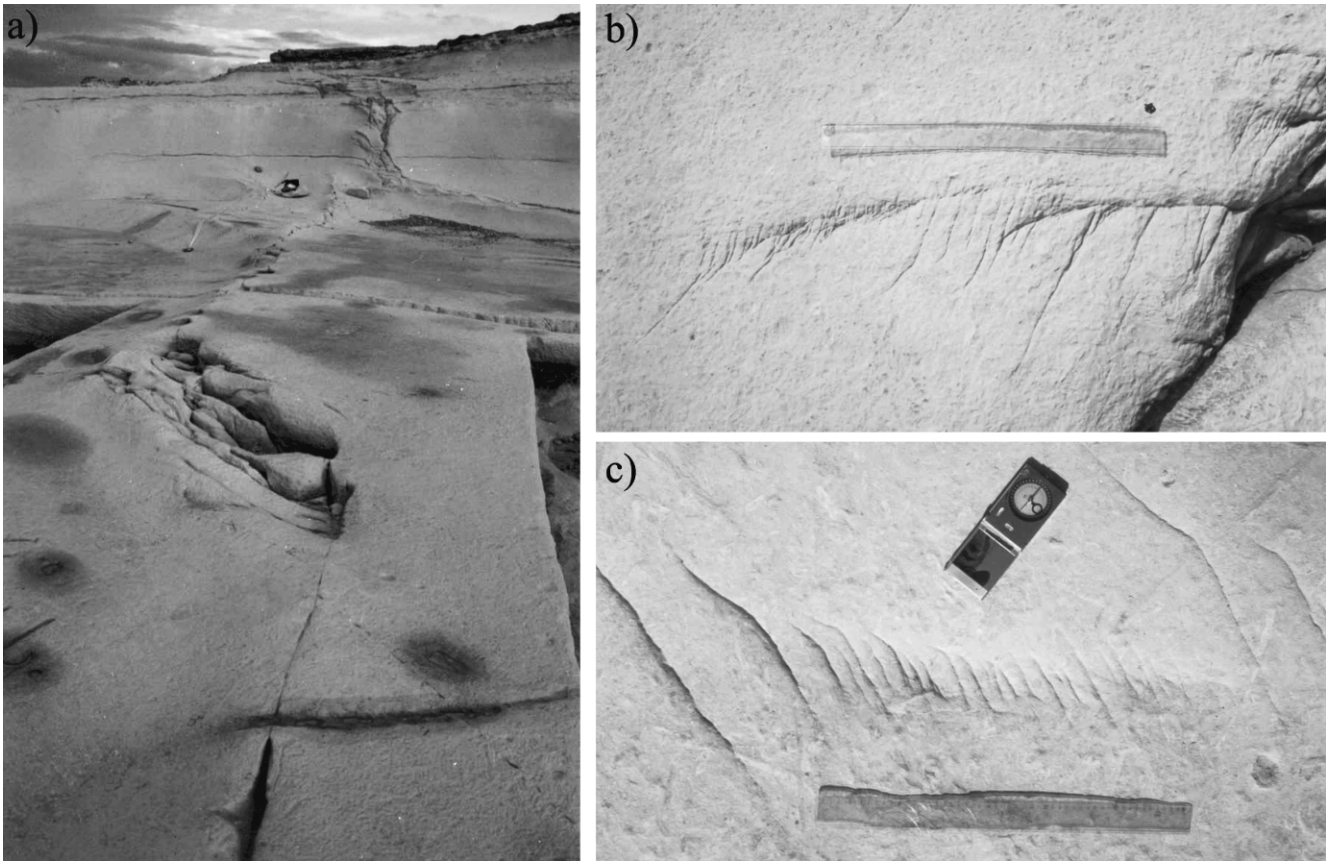

Fig. 2. Photographs of strike-slip faults and damage zones to the west of Marsalforn, Gozo Island. (a) A strike-slip fault zone with a linking damage zone in the form of a pull-apart. The view direction is towards the SE, which is along the strike of the major faults. A map of this structure is shown in Fig. 8. (b) Damage zone at a tip of a left-lateral strike-slip fault, with a wedge-shaped damage pattern with antithetic and branching faults. Similar damage zones are shown in Figs. 5–7. (c) A distributed damage zone showing several antithetic fault segments and tip cracks. A map of this structure is shown in Fig. 12a. The 0.5-m-ruler in (b) and (c) is for scale.

extension fractures are steeply dipping (>70°), with a stereogram shown in Fig. 3b. Strikes of right-lateral faults range from N020° to N080° (with a modal strike of N045°), left-lateral strike-slip faults range from N070° to N130° (mode N100°), and extension fractures from N050° to N090° (mode 070°). The average azimuth of the maximum compressive stress (σ_1) is therefore inferred to have been ~N070°. The orientation data of faults and fractures indicate a conjugate strike-slip fault set and secondary fractures.

To examine the angular relationships of master faults to secondary faults and extension fractures, the orientation data were plotted in terms of the adjacent master fault traces (Fig. 3c). Since most of the data were collected from left-lateral faults, data collected from right-lateral faults have been reflected about a horizontal plane to show the general relationship to master faults. Positive angles are here measured anti-clockwise from left-lateral faults. Faults (mode II/III) typically occur at 30° to −20° (synthetic faults) and at 60–100° (antithetic faults) to the overall orientation of the fault zone, and generally have no vein filling. Extension fractures are mode I fractures developed as joints (unfilled) or veins (calcite filled), and occur at 30–60° to the faults (Fig. 3c). Faults commonly develop wing cracks oblique to the fault plane (e.g. Pollard and Segall, 1987), while extension fractures (~45°) propagate parallel to their planes.

Displacement markers are rare because the faults are exposed on bedding planes, but displacement magnitudes can be measured from the offset of trace fossils or early

Fig. 3. (a) Strikes of faults and extension fractures in the study area. Right-lateral strike-slip faults range from N030° to N070°, left-lateral strike-slip faults range from N060° to N120° and extension fractures are concentrated between N060° and N080°. The inferred azimuth of σ_1 is about N070°. (b) Equal area stereographic projection, including 27 major faults, and 13 secondary faults and extension fractures. The mean strike/dip of the left-lateral faults and secondary faults is N85°W/84°NE, while the mean strike/dip of the right-lateral faults is N48°E/87°N. The mean strike/dip of the extension fractures is N68°E/85°N. (c) Angular relationship of fractures to master faults. Positive (+) values indicate strikes anticlockwise from each master fault, and negative (−) values indicate strikes clockwise from each master fault for left-lateral strike-slip. Data from right-lateral faults are reflected about a horizontal plane.

a)

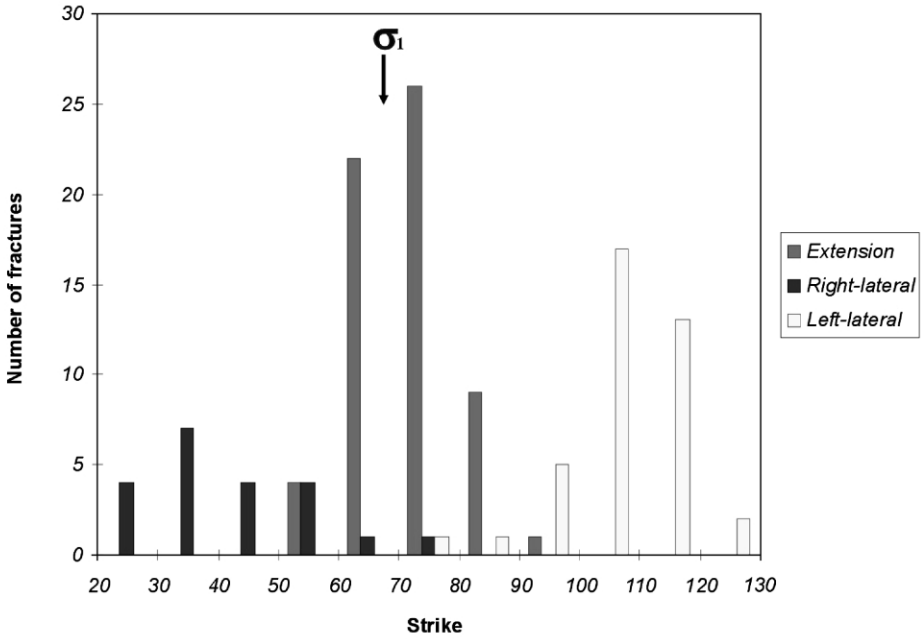
σ1
Number of fractures
Strike
Extension
Right-lateral
Left-lateral

b)

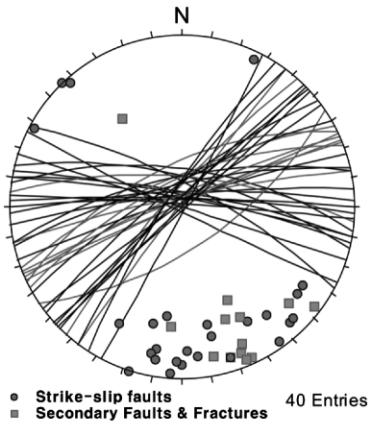
N
Strike-slip faults
Secondary Faults & Fractures
40 Entries

c)

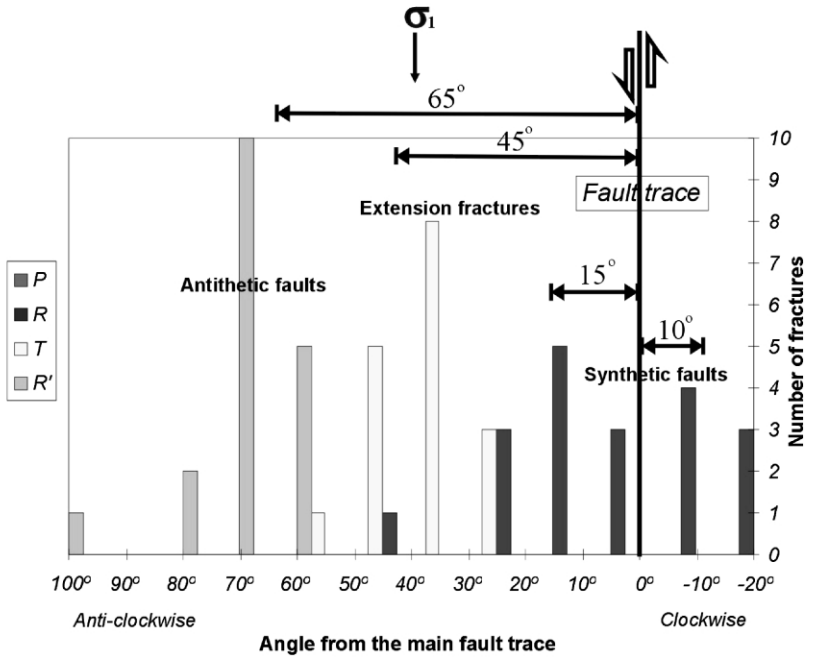
σ1
65°
45°
Fault trace
Extension fractures
Antithetic faults
15°
10°
Synthetic faults
P
R
T
R'
Number of fractures
Anti-clockwise
Clockwise
Angle from the main fault trace

fractures, and from the width of pull-aparts. No unambiguous slickenside lineations were observed, with the strike-slip sense of displacement being indicated by the absence of vertical displacement of beds and by the geometries of pull-aparts. These indicate dominantly strike-slip (horizontal) displacements of up to 220 mm. It can be difficult to distinguish the shear senses of fractures within damage zones. Some studies identified antithetic faults in damage zones (e.g. Tchalenko, 1970; Tchalenko and Ambraseys, 1970; Davis et al., 2000), whereas other researchers have described extension fractures (e.g. Segall and Pollard, 1983; Harding et al., 1985; Moore and Lockner, 1995; Mollema and Antonellini, 1999). Although some of the fractures do not show unambiguous displacement sense indicators, some of the fracture tips are bent or generate higher order (smaller) tip cracks, indicating the displacement sense.

3. Damage zones at fault tips

3.1. Tip damage zones dominated by extension fractures

Fig. 4 shows two left-lateral fault zones striking N110°–N125° with extension fractures at fault tips. The extension fractures strike ~N070°, which is parallel to the inferred regional σ_1. Short (<0.5 m) extension fractures, striking N076°, are developed around the fault tip shown in Fig. 4a, and generally decrease in length towards the fault tip. A series of short (<0.5 m) extension fractures occur along the fault shown in Fig. 4b, mainly in the extensional quadrant. This type of tip damage zone shows extension fractures that are either attached singly to the fault and so resemble *wing cracks* (Fletcher and Pollard, 1981; Rispoli, 1981; Pollard and Segall, 1987), or multiply where they resemble the *horsetails* (Granier, 1985; Kim et al., 2001). The angle between the master fault and the extension fractures is generally ~40°, although higher angles can occur. Extension fractures are commonly slightly curviplanar and show little additional fracturing at their tips.

3.2. Tip damage zones dominated by antithetic faults

Wedge-shaped damage zones are commonly developed at fault tips (Figs. 5 and 6). The size of the wedge is generally proportional to fault length. The most common fractures in this type of damage zone are second order antithetic faults at 60–70° to the master fault, with some extension fractures occurring (also see McGrath and Davison, 1995, fig. 11). The displacement sense of the antithetic faults can be inferred from the displacement of earlier fractures, from their angle to the master fault, and from the tip cracks, which open up at approximately 45° to the antithetic faults. Several second-order synthetic faults link the second-order antithetic faults, with these synthetic faults and extension fractures tending to be shorter and less frequent than the antithetic faults. Some antithetic faults

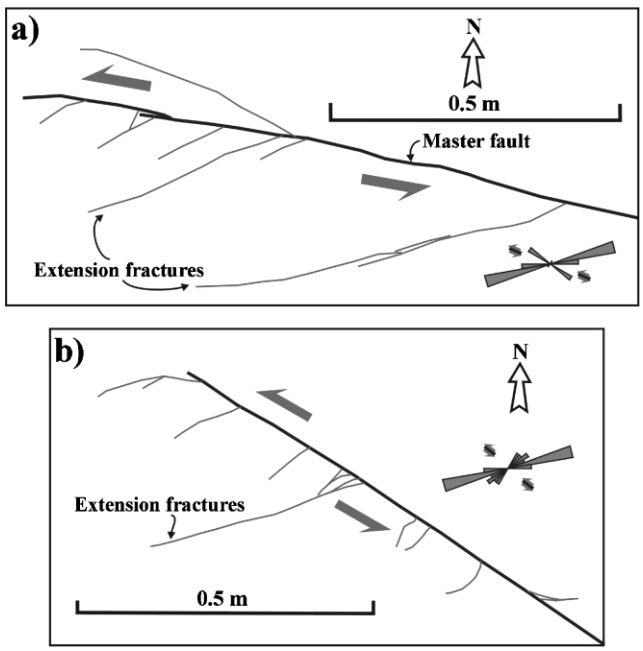

Fig. 4. Left-lateral faults showing branching faults or extension fractures at fault tips. (a) The strike of the master left-lateral strike-slip fault is N110°, and the mapped damage zone is about 1 m long. Most of the branching faults are developed in the extensional quadrant. (b) An 8 m long left-lateral fault striking about N125°, with a 1 m long damage zone, in which tip fractures strike around N070° and N040°.

show smooth sigmoidal shapes, indicating the overall displacement sense of the fault zone and that rotation has occurred.

Some of the damage zones show a rotation in strike away from extensional quadrant toward the contractional quadrant. This phenomenon is more obvious in larger fault zones (e.g. Figs. 5 and 6a), and may be attributed to shear at the cohesive end zone (e.g. Cowie and Scholz, 1992; Martel and Boger, 1998). The fault tip shown in Fig. 6c has antithetic faults and branching synthetic faults or extension fractures that combine to form a wedge-shaped damage zone. Most of the antithetic faults are in the extensional quadrant, and the trace of the master fault bends towards the extensional quadrant.

3.3. Tip damage zones dominated by antithetic faults and extension fractures

The antithetic faults shown in Fig. 7 show several extension fractures with smaller antithetic faults. Antithetic faults dominate away from the tip of the master fault, with several wedge-shaped zones of higher order (i.e. smaller) antithetic faults developed at some fault tips. Several second-order synthetic faults crosscut antithetic faults (Fig. 7). Various studies (McKinstry, 1953; Moody and Hill, 1956; Chinnery, 1966b; Arboleya and Engelder, 1995; Willemse et al., 1997; Davis et al., 2000) have described higher-order faults and extension fractures, which are similar to those developed around secondary antithetic faults in the study area (Figs. 5–7).

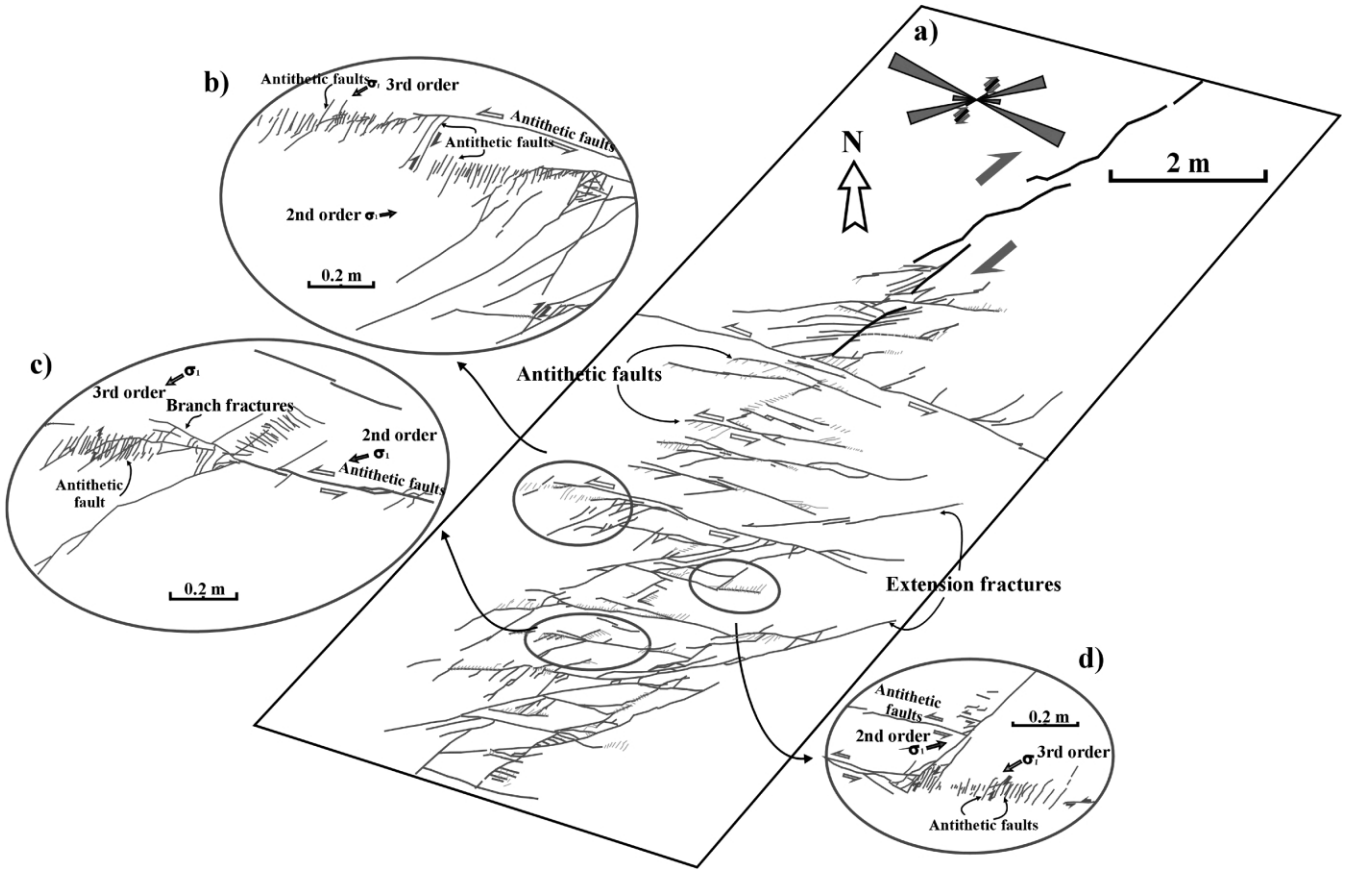

Fig. 5. (a) Map of a tip damage zone from a right-lateral fault striking N044°, showing two orders of secondary fracturing. The master fault has a trace length of about 19 m, and the mapped damage zone extends for about 10 m from the fault tip. The dominant structures in the tip region are antithetic faults striking N110°–N120°. Branching synthetic faults and extension fractures striking N070°–N080° also occur, but tend to be shorter and less frequent. (b)–(d) Detailed maps of the damage zone.

4. Damage zones at fault linkages

4.1. Linking damage zones dominated by extension fractures

The fault shown in Fig. 8 consists of several left-lateral fault segments linked through highly fractured extensional oversteps (also see Martel et al., 1988). The measured maximum displacement of the fault zone from the offset of burrows is ~220 mm. The extensional oversteps are dominated by extension fractures and pull-aparts striking N060° ~ N080°, i.e. at 40–50° to the master fault zone. Some of these fractures, particularly within the extensional oversteps, are partially filled with calcite. H-shaped bridge patterns, where younger fractures abut older ones (Hancock, 1985), provide evidence of the secondary extension of oversteps (Gamond, 1987; Peacock, 2001). Although extensional oversteps are dominant, some minor contractional overstep zones occur between fault segments (Fig. 8).

4.2. Linking damage zones dominated by antithetic faults and branching fractures

This style of damage zones is most commonly developed between two sub-parallel fault segments that understep and that are coplanar or slightly non-coplanar (Fig. 9). A series of branching fractures extend between the understepping faults to produce a damage zone occupied mainly by antithetic faults at a high angle to the branching fractures. Some of the branching fractures terminate against antithetic faults and vice versa, suggesting they were contemporaneously active. There is a tendency for block rotation within the damage zones between two sub-parallel faults that understep (Rispoli, 1981).

4.3. Pull-aparts

Stepping master faults are commonly linked by pull-aparts (e.g. Crowell, 1974; Rodgers, 1980; Connolly and Cosgrove, 1999). Fig. 10a and b shows pull-aparts developed along an E–W striking left-lateral fault zone. The sense and magnitude of displacement on the faults is indicated by the widths of pull-aparts. In the example shown in Fig. 10a, the linking fractures are synthetic to the master faults, whereas linkage of the master faults is via extension fractures in the example shown in Fig. 10b. Faults that terminate at extension fractures probably post-date the extension fractures (Segall and Pollard, 1983; Hancock, 1985). Gamond (1983) and

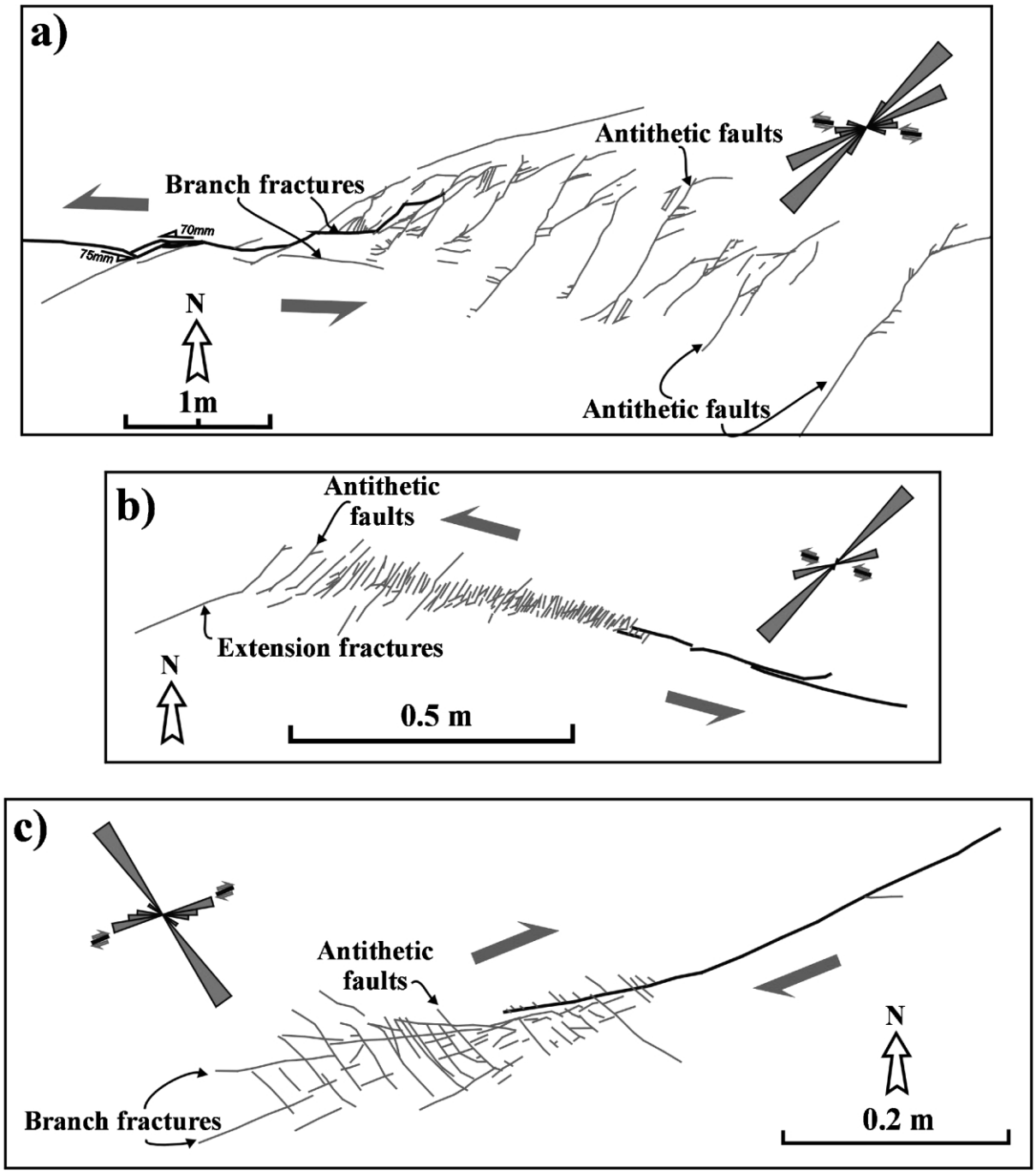

Fig. 6. Damage at fault tips dominated by wedge-shaped zones of antithetic faults, with both the length and spacing of antithetic faults increasing away from the fault tip. (a) Left-lateral strike-slip fault striking N100°. (b) Left-lateral fault tip striking about N110°. (c) Right-lateral fault that bends towards the extensional quadrant at the tip.

Peacock and Sanderson (1995b) described similar geometries of pull-aparts. The pull-apart shape caused by the linkage of differently orientated sets of synthetic faults (Fig. 10a) is a relatively long narrow trapezoid, whereas linkage of synthetic faults and extension fractures (Fig. 10b) produce a wide trapezoid with a higher intersection angle. Linkage of faults at pull-aparts produces fault zones with kinked or zigzagged traces.

5. Distributed damage zones

Some of the faults at Marsalforn appear to be reactivated joints (Peacock, 2001), so fault damage tends to be concentrated at their tips (also see Martel et al., 1988). Distributed damage is, however, developed along most of the fault zone, generally producing relatively long, narrow zones with en échelon fractures with similar length and spacing arranged symmetrically about the fault. Such

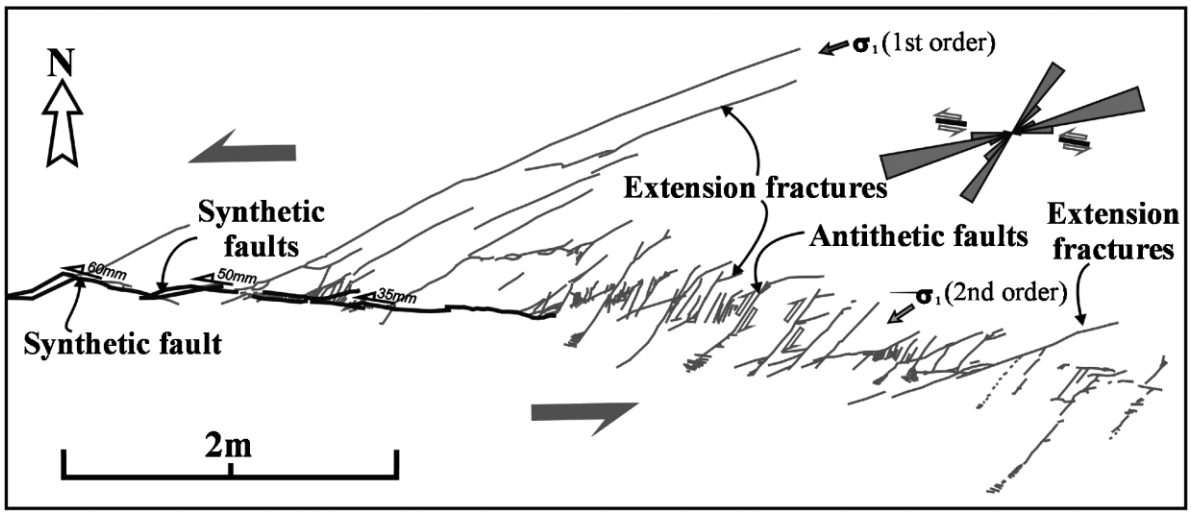

Fig. 7. Damage zone about 6 m long at the tip of a left-lateral strike-slip fault. The segmented master fault strikes about N100°, with antithetic faults and extension fractures striking about N040° and N070°, respectively.

damage zones have been widely described from zones of simple shear (e.g. Tchalenko, 1970; Tchalenko and Ambraseys, 1970; Wilcox et al., 1973; Bartlett et al., 1981; Christie-Blick and Biddle, 1985; Caine and Forster, 1999; Davis et al., 2000). Distributed damage zones that consist of en échelon fractures can be divided into those dominated by extension fractures (Fig. 11) and those dominated by antithetic faults (Fig. 12).

5.1. Distributed damage zones dominated by extension fractures

Damage zones dominated by extension fractures are relatively long and wide, with extension fractures rarely having tip cracks and forming at 30–40° to the master faults. Some fractures do display tip cracks and sigmoidal shapes, and these are interpreted as early extension fractures that have experienced some subsequent shear and rotation. Fig. 11 shows fault zones that consist of en échelon extension fractures, with little additional damage, e.g. limited development of antithetic faults in the central parts of the fault zones. In both cases, the mean strike of the left-lateral master fault is ~N100° and extension fractures form at ~N070° (i.e. at about 30° to the master fault), which is sub-parallel to the inferred regional σ_1 (Fig. 3a). Some extension fractures curve to make a smaller angle to the master fault as they extend away from the fault plane.

Fig. 11a shows a fault zone that consists of en échelon extension fractures with no central master fault. Some of the extension fractures have kinked tips or show sigmoidal shapes, suggesting later shear and rotation, and are linked by short synthetic faults developed in the centre of the zone. The fault zone shown in Fig. 11b is straight, with a small contractional overstep in the middle of the fault zone.

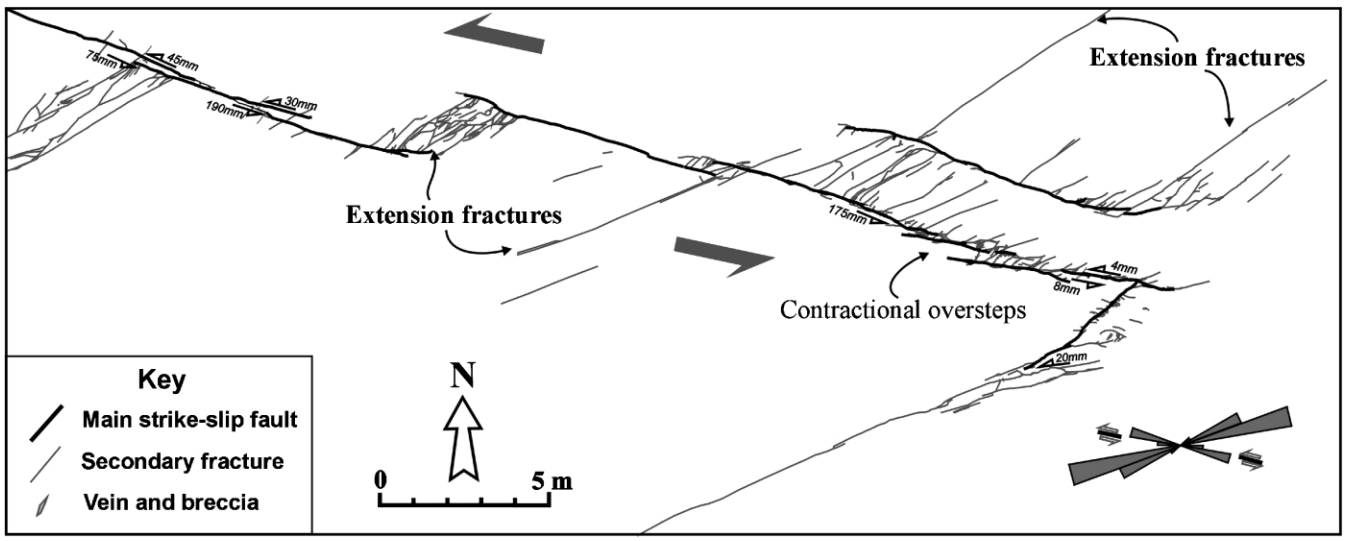

Fig. 8. Map of a left-lateral strike-slip fault zone with a trace length of over 30 m, consisting of several sub-parallel fault segments (average strike N108°). The segments are mainly linked through mostly extensional oversteps, within which high intensities of secondary extension fractures are developed.

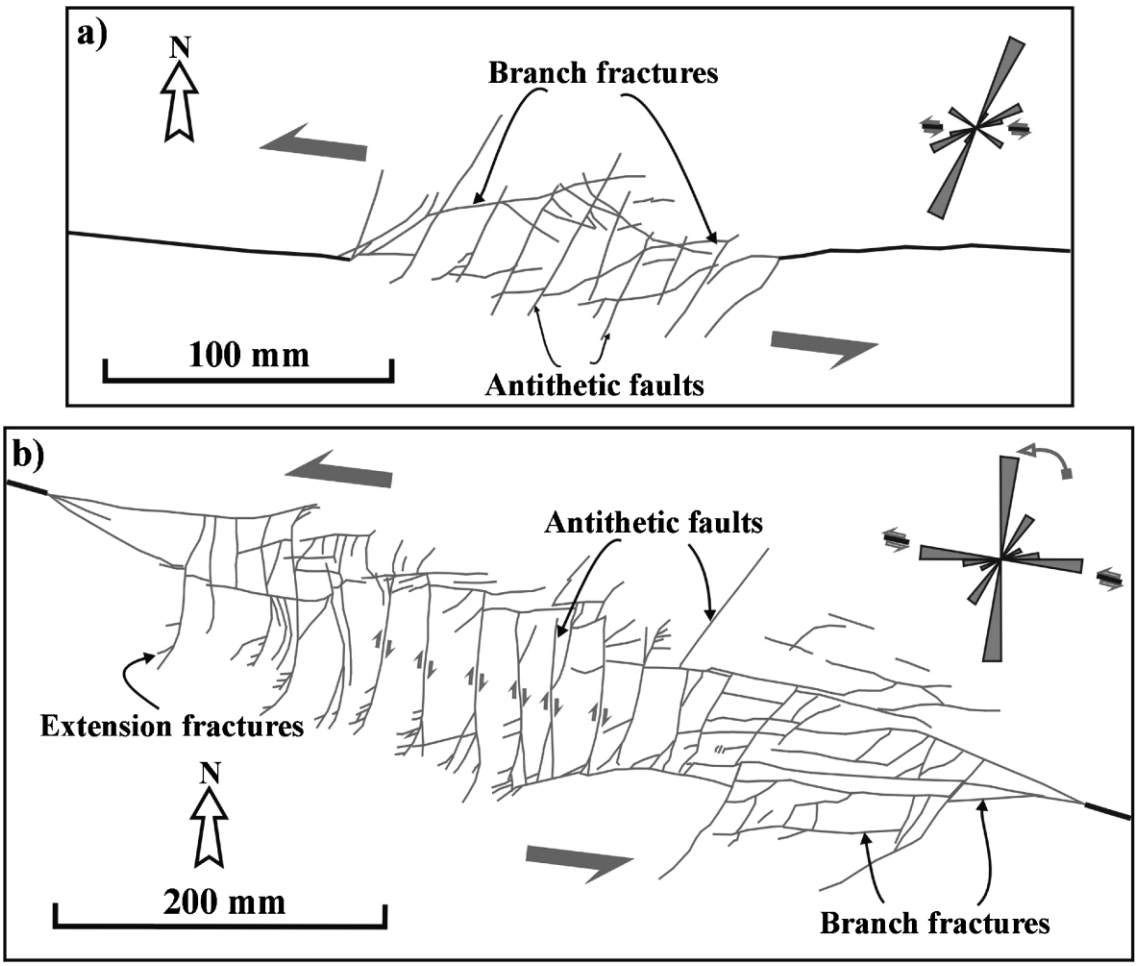

Fig. 9. Maps showing left-lateral strike-slip fault zones with tip damage zones between understepping fault segments. (a) A 150-mm-long overstepping tip damage zone between two E–W striking faults. Antithetic faults strike N028°, and splay fractures range from N060° to N120°. (b) A complex, linking damage zone between sub-parallel left-lateral faults, in which antithetic faults terminate against branching synthetic faults. These define a series of rotated blocks, with the antithetic faults rotated to an almost N–S strike.

Damage occurs at the eastern tip, which is dominated by antithetic faults. There is a difference of 10–20° between the extension fractures in the wall zone and at the western tip of the fault zone, suggesting different local stresses were responsible for their generation.

5.2. Distributed damage zones dominated by synthetic and antithetic faults

Damage zones dominated by antithetic faults are relatively short and narrow, with fractures commonly having tip cracks and forming at ~65° to the master faults. The damage zones illustrated in Fig. 12 are long, narrow, approximately symmetric areas, with no through-going fault, although some fault segments occur. In most examples (e.g. Fig. 12b and c), short synthetic fault segments occur, but these are absent in the example shown in Fig. 12a. Several straight fault segments occur in the central part of some fault zones, where there are few antithetic faults around fault segments (Fig. 12c). These segments are aligned and linked through oversteps with more intensive antithetic faults. Many high-angle antithetic faults occur at about +65° to the fault zone, these dominating along the whole fault zone. Most of the antithetic faults are of similar length and tend to be uniformly spaced along the fault zone (e.g. Fig. 12b). This, together with the absence of obvious wedge-shaped patterns, is very different from the tip damage discussed in Section 3, although some along-strike fault tips may be overprinted (Fig. 12c). Later synthetic faults cut and displace some of the antithetic faults.

6. Cross-sections of strike-slip fault tips

There are several cliff sections through strike-slip fault zones near Marsalforn (Fig. 13). When combined with map views, these cliff sections give insights into the 3D geometry of the strike-slip fault zones. Both faults illustrated in Fig. 13 show branching fractures that diverge

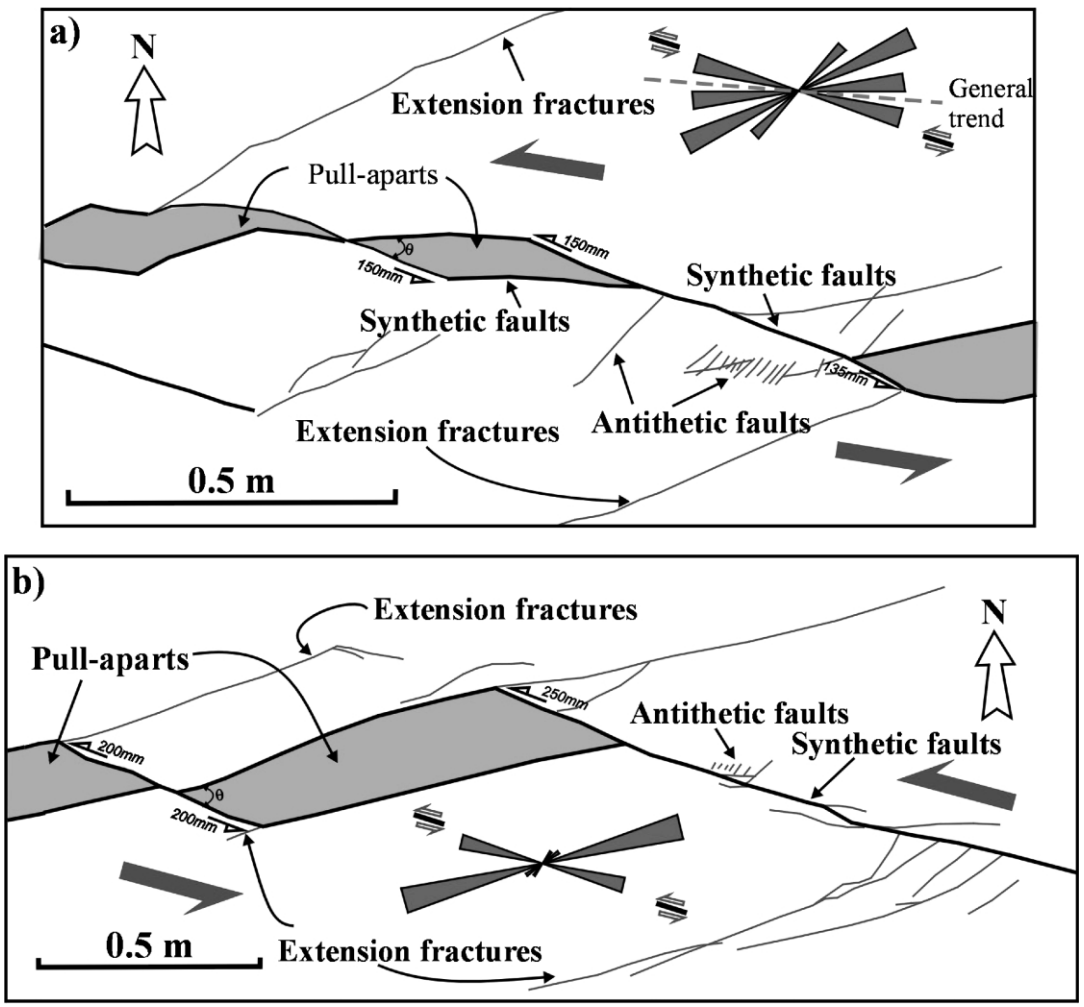

Fig. 10. Maps of two left-lateral faults showing zigzag geometries with pull-aparts. (a) A fault zone consisting of several secondary faults, with pull-aparts developed by displacement on synthetic faults at about 20° to the fault zone and by opening of synthetic faults that are approximately parallel to the fault zone. (b) A fault zone with pull-aparts developed by displacement on synthetic faults that are at about 20° to the fault zone and by opening on extension fractures.

upwards from the fault tips to produce cone-shaped damage zones in which the number of fractures decreases downwards. The fault in Fig. 13a shows a damage zone that is asymmetric about the master fault, whereas the fault in Fig. 13b shows a slightly higher intensity of sub-horizontal fractures on the NW side, but the damage geometry is almost symmetric on either side of the master fault. The main fractures branching from the master fault tips are probably synthetic faults, based on their strike (Fig. 13). The faults shown in Fig. 12b and c show en échelon synthetic faults that may also represent the up- or down-dip fault tip breaking through to form a through-going fault.

These cone-shaped damage zones have similar geometries to *flower structures* (Wilcox et al., 1973; Sylvester and Smith, 1976; Bartlett et al., 1981; Sylvester, 1988) and to the up-dip tip of a strike-slip fault exhibiting a series of bifurcating fractures observed by McGrath and Davison (1995). Naylor et al. (1986) reported an analogous structure in seismic section.

7. Interpretation of the damage zones at Marsalforn

7.1. Development of damage zones

Extension fractures commonly form before the generation of a through-going fault (e.g. Fig. 11a). Reches and Lockner (1994) and Moore and Lockner (1995) showed that extension fractures formed in laboratory experiments prior to the nucleation of a fault are sub-parallel to σ_1, whereas those generated in the tip zone make angles of about 20° to the far-field σ_1. Extension fractures striking N070°, parallel to the regional σ_1, might therefore be developed in the early stages (Cox and Scholz, 1988), whereas those at fault tips developed to accommodate the displacement along the fault at a later stage.

The inferred stress axes for higher-order fault sets differ systematically from those of the lower-order faults (e.g. Fig. 14). The pattern can be explained assuming that the higher-order antithetic faults (dominant) form at 65° to the master fault and that there is a 15° rotation of σ_1 at each fault tip.

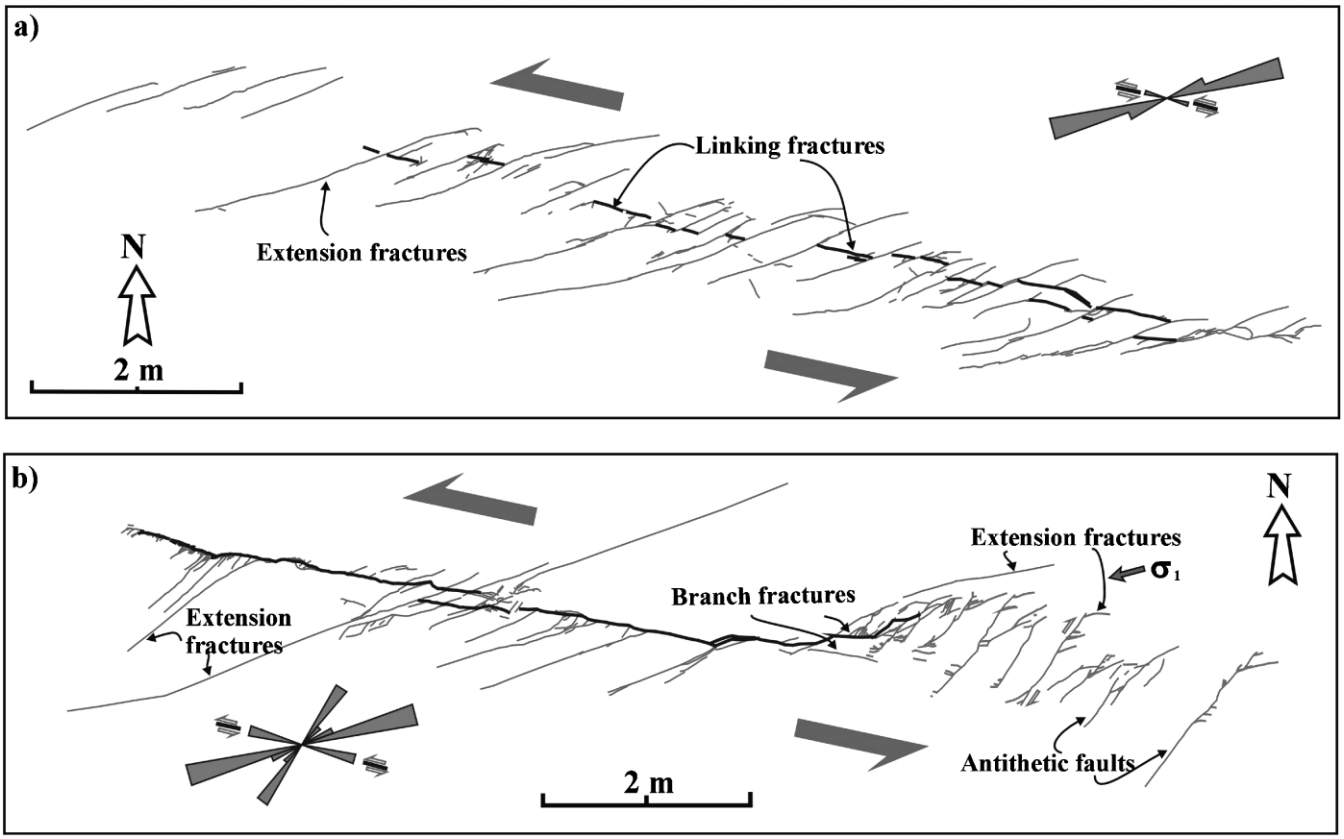

Fig. 11. Maps of damage zones that are dominated by extension fractures. (a) A 12 m long fault zone that strikes N102°, with predominantly extension fractures striking N070°, some of which are linked by synthetic faults that are sub-parallel to the fault zone. This pattern is similar to fracture patterns produced in experimental studies by Cox and Scholz (1988). (b) A 13 m long left-lateral strike-slip fault striking N100°, with several secondary extension fractures and a wedge-shaped tip zone dominated by antithetic faults.

Displacement along a fault generates a shear-induced stress that results in a rotation of the sub-regional direction of σ_1 into a local direction of σ_1 (Mandl, 1988; Davis et al., 2000). The examples shown in Fig. 9 illustrate fracture evolution within linkage zones at Marsalforn. Antithetic faults initiated at about 70° to the master faults (as in Fig. 9a) and then rotated to about 100° as block rotation developed (Fig. 9b; Schreurs, 1994). The antithetic faults acquired a sigmoidal shape and usually terminated against earlier faults.

In distributed damage zones dominated by antithetic faults, the long, narrow, symmetric damage zone and the absence of a through-going fault suggest stress distribution related to a mode III fault tip above or below the location of exposure (Fig. 12a–c). Some of the en échelon fractures evolve into mode III tip damage (Fig. 12b and c; Martel and Boger, 1998).

Antithetic faults are rare in the walls of fault segments (e.g. Fig. 12c). Tchalenko (1970) suggested that antithetic faults tend to become passive and distorted into an S shape as displacement develops. If a through-going fault propagates across the damage zone, any early-formed antithetic faults may be inhibited by localisation of displacement along the fault segments. Antithetic faults are, however, abundant at fault oversteps (Fig. 12b and c; Davis et al., 2000), and indicate where faults have propagated by linkage of segments (Kim et al., 2000). Several fault segments start to develop in the central part of the distributed damage zones. They initiate from small linking fractures (Fig. 12a) and evolve through en échelon synthetic faults (Fig. 12b), to eventually form linked faults with zigzag traces. This evolutionary sequence (Fig. 12a–c) suggests that many zones of distributed damage may represent mode III tips. The damage zone illustrated in Fig. 12c is more typical as fault displacement increases, where initial mode III tip damage has been cut by fault segments, which link to produce a fault with mode II tip pattern at the fault tips. At the tips of fault segments, the damage is complicated due to a combination of mode II and III tips. The relicts of antithetic faults along the fault and the linked zigzag geometry (Bilham and Williams, 1985; Moore and Lockner, 1995) of the fault trace are evidence for this evolution.

7.2. Models for the evolution of strike-slip faults on Gozo

In this section, three models of fault propagation are proposed for the strike-slip faults at Marsalforn (Fig. 15). We consider these models to apply to different locations on the fault plane.

In the first model, faults initiate from en échelon

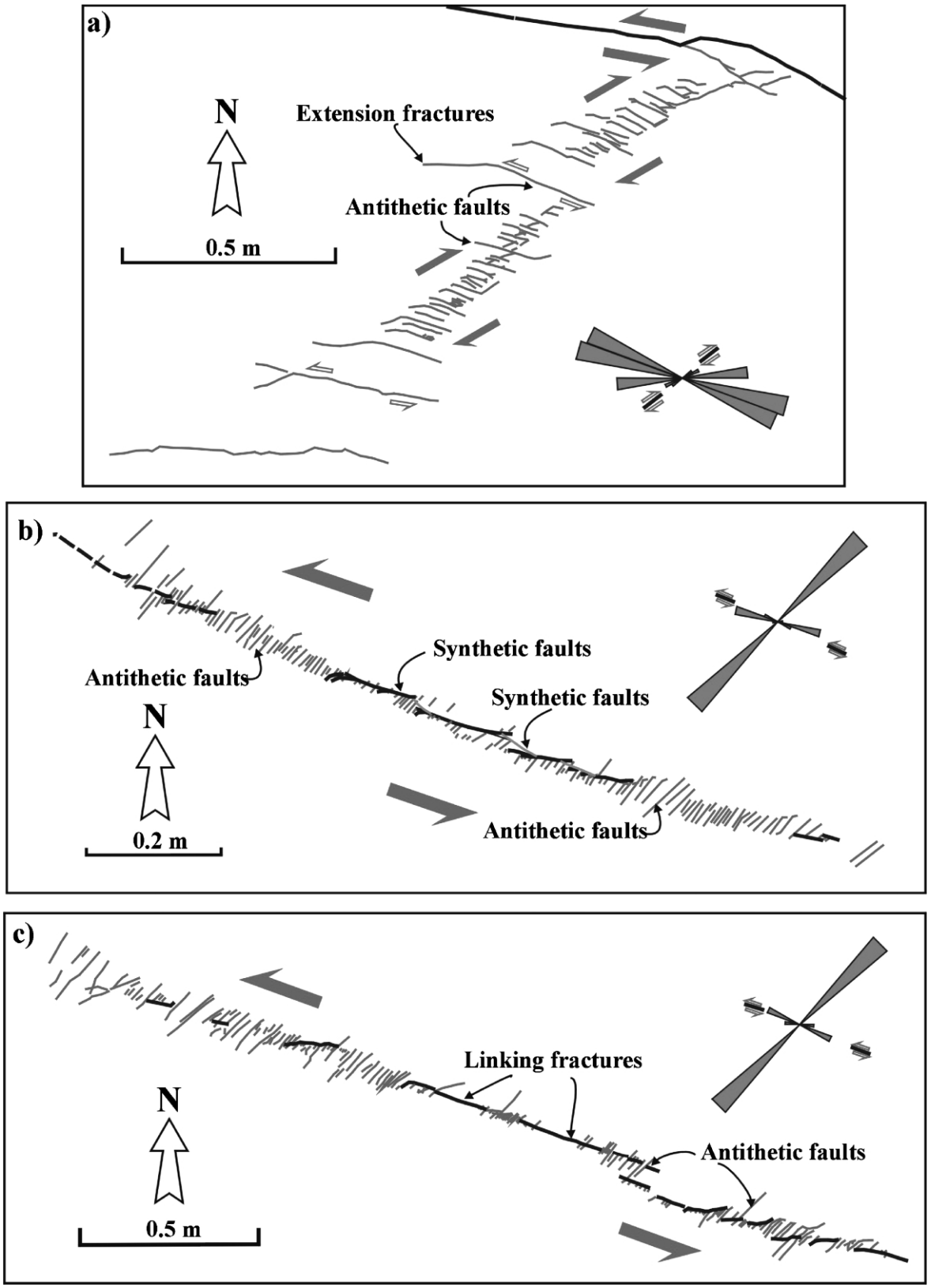

Fig. 12. Maps showing zones of distributed damage along faults. (a) A 2 m long right-lateral fault zone (strike N058°) dominated by antithetic faults. (b) A segmented left-lateral fault (strike N115°) with associated damage zone in which en échelon antithetic faults (strike N045°) predominate. Some fault segments are linked by synthetic faults. (c) A left-lateral fault (strike N112°) with damage zones consisting of en échelon antithetic faults (strike N050°).

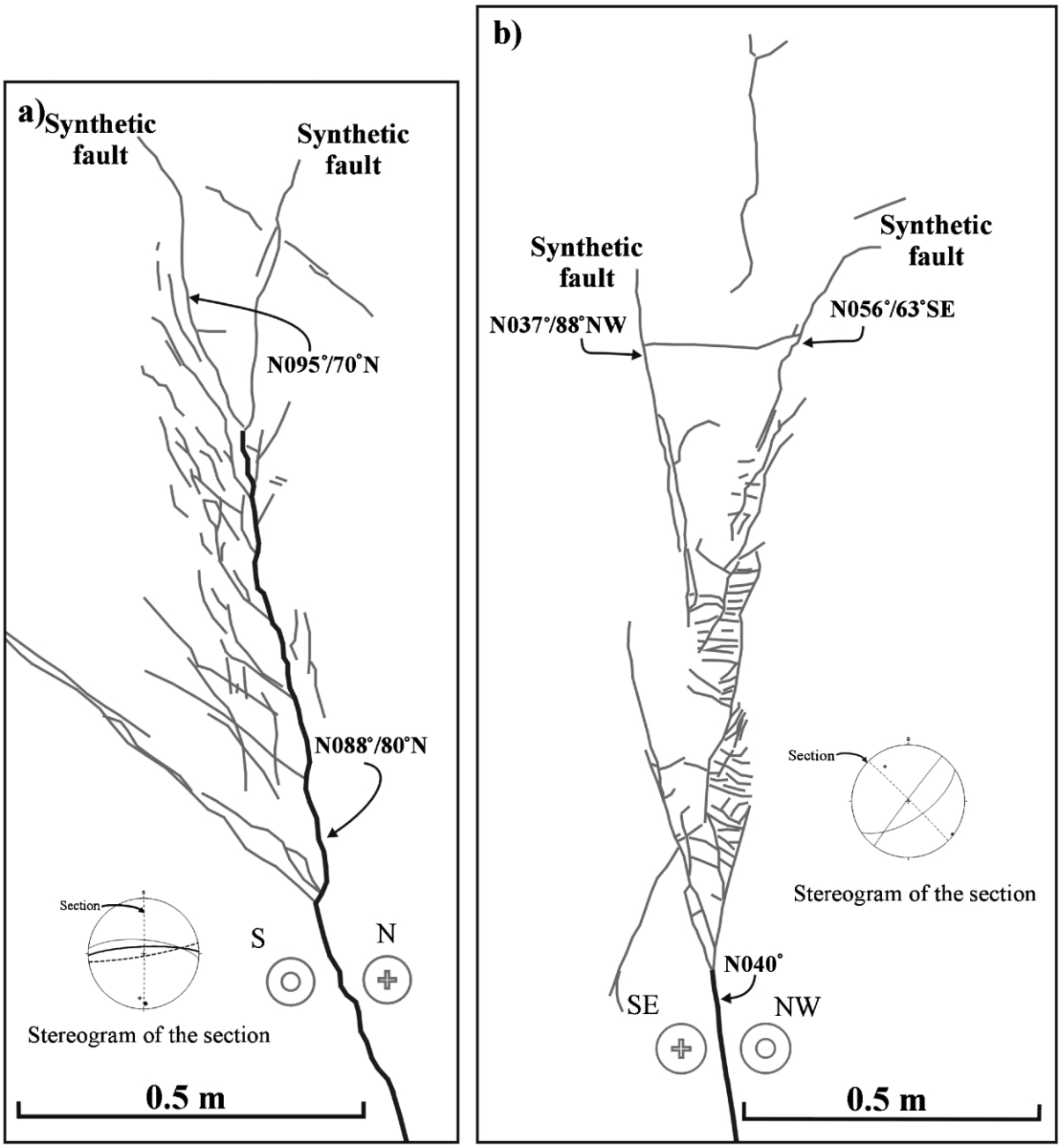

Fig. 13. Vertical cross-sections of the up-dip tips of strike-slip faults. (a) A left-lateral fault (dipping N088°/80°NW) with an asymmetric damage zone. Most fractures developed on the south side of the fault, but are more symmetrical above the fault tip. (b) A right-lateral fault (strike N040°E), with a 1.5 m long damage zone that includes flat-lying linking fractures.

extension fractures (Fig. 15a), which mechanically interact and link to generate a fault (Cox and Scholz, 1988; Martel et al., 1988; Reches and Lockner, 1994; Mollema and Antonellini, 1999; Peacock, 2001). Cox and Scholz (1988, fig. 9) produced a fracture pattern that is analogous to the fracture patterns illustrated in Fig. 11a. They attribute extension fractures to the initial stress field, with linking fractures forming later as the deformation increased. Secondary fractures, which include synthetic faults, link to form a through-going master fault (Figs. 8 and 11b). Extension fractures are generally parallel to the σ_1 direction, whereas faults are orientated obliquely to σ_1 (e.g. Scholz, 1968; Naylor et al., 1986).

The second model (Fig. 15b) involves the growth of mode II fault tips by the linkage of tip cracks (Peacock, 1991; Cartwright et al., 1995; Moore and Lockner, 1995; Kim et al., 2000) producing a zigzag fault trace. Faults link through secondary fractures and the breaching of oversteps (e.g. Figs. 8 and 9). Examples have been documented from microscopic scales (Moore and Lockner, 1995) to regional scales (Bilham and Williams, 1985).

The third model (Fig. 15c) follows the classical Riedel

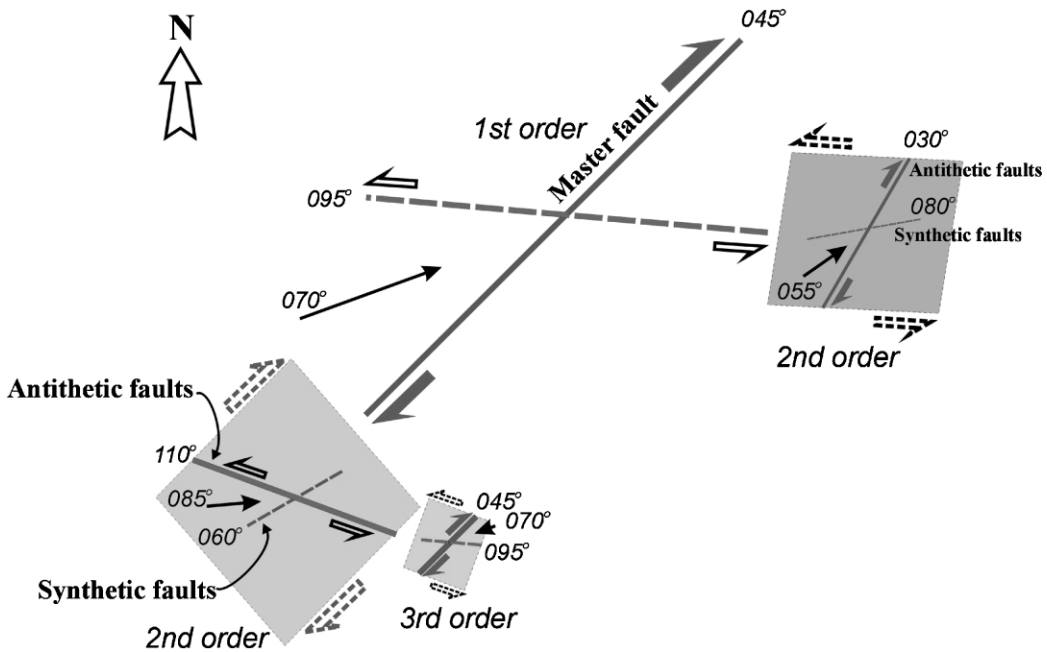

Fig. 14. Typical geometries of faults developed over three orders of magnitude in strike-slip faults. Note the change in orientation of σ_1 (arrow) and the switch in displacement sense of the dominant faults (continuous lines). The dashed lines represent the synthetic fault set at each size order.

fracture pattern (e.g. Tchalenko, 1970; Wilcox et al., 1973; Bartlett et al., 1981). For early synthetic and antithetic faults, σ_1 lies within a horizontal plane at about 45° to the imposed shear direction (Schreurs, 1994). The synthetic and antithetic faults are both unfavourably orientated to sustain large displacements, and further straining must take place to accommodate increased displacement (Tchalenko, 1970). Several models (Morgenstern and Tchalenko, 1967; Gamond, 1983, 1987; Swanson, 1988; Sims et al., 1999) have shown that such fault zones are composed of first-generation fractures of the Riedel type, linked by second-generation synthetic faults that are sub-parallel to the fault zone. The antithetic faults commonly respond passively by rotation and distortion (Fig. 9b), being nearly at right angles to the general displacement direction. The combination of extension fractures and displacement along the synthetic faults leads to the formation of zigzag-shaped fault traces orientated in the general direction of displacement (Fig. 10). Pull-aparts are generally formed by the combination of any two of the fracture sets (antithetic, synthetic, fault zone parallel faults, or extension fractures).

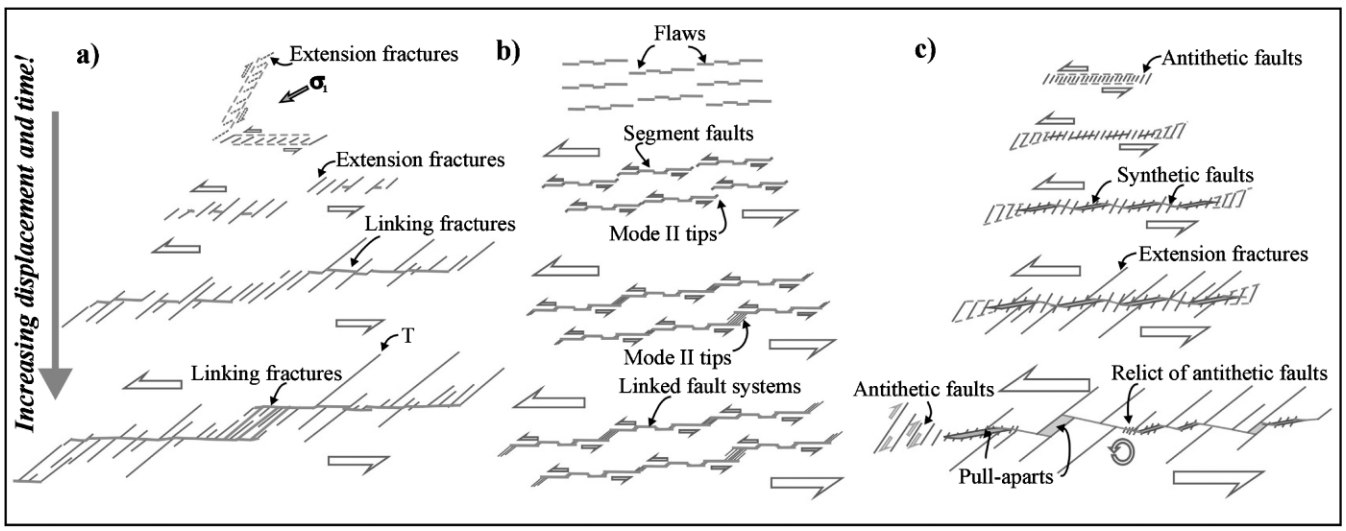

Fig. 15. Simple models for the evolution of small displacement strike-slip faults. (a) A fault system dominated by extension fractures, linked by later fault segments that are sub-parallel to the fault zone. (b) A system of along-strike (mode II) tips linked by later secondary fractures (see Martel et al., 1988). (c) A system dominated by the early generation of antithetic faults intersected by later synthetic faults, with extension fractures dominating at a later stage.

7.3. 3D model of a strike-slip fault and its damage zones

The damage zone types described here have been classified in terms of their locations along faults, such as tip zone (tip damage), wall zone (distributed damage), and linkage zone (linking damage). The fracture type is mainly determined from displacement senses inferred from displaced markers, pull-apart geometries, wing cracks, tip patterns (such as curvature), angles between strikes of the major fault and secondary fractures, and fracture patterns in relation to the strike of the fault zone.

It is also possible to interpret the damage zones at Marsalforn in terms of their position on a fault tip line in 3D. An along-strike tip of a strike-slip fault is a mode II tip, whereas an up- or down-dip tip is a mode III tip (Lawn, 1993; McGrath and Davison, 1995). Numerical models indicate that the stress concentration at a propagating mode II tip is asymmetric across the fault plane, with extensional and contractional quadrants (e.g. Segall and Pollard, 1980; Pollard and Segall, 1987; Reches and Lockner, 1994), whereas the stress concentration for mode III tips is symmetrical across the fault trace (Pollard and Segall, 1987). Because of these differences, the orientations of damage zones and the geometries of associated fractures are different at different locations on a fault tip line. It is therefore possible that we can recognise where we are on a fault plane from the nature and geometry of the damage zones.

We suggest that damage zone geometries and associated fracture patterns will be different depending on both the location around a strike-slip fault plane and on the fault evolution stage. 3D models for a strike-slip fault with two tip modes (II and III) (Fig. 16) and for a linked strike-slip faults (Fig. 17) have been developed, based on geometries of damage zones observed on Gozo. The model shows different styles of damage zones at different horizontal cross-sections through the fault (Figs. 16A–D and 17A and B), and a simple vertical cross-section with mode III tip damage (Fig. 16E).

Extension fractures are first to initiate (Fig. 16C and D; e.g. Cox and Scholz, 1988; Reches and Lockner, 1994; Mollema and Antonellini, 1999), and en échelon extension fractures link to produce a fault (Willemse et al., 1997). Most of these extension fractures are long and straight, and are displaced by the master fault without tip cracks. Another type of extension fracture is localised at mode II tips, forming *wing cracks* or *horsetails*. The orientation of extension fractures at mode II fault tips is controlled by local stress redistribution and is slightly different in orientation and location from the extension fractures elsewhere in the wall-rocks (Moore and Lockner, 1995; Petit and Mattauer, 1995).

Antithetic faults are usually the first fractures to appear in a fault zone that propagates upwards, if we observe the unexposed fault from the top (Fig. 16A; e.g. Tchalenko, 1970). This may be considered as a mode III tip of a master fault. The large angles (~65°) of antithetic faults to the general displacement direction, shown at the early stage of a mode III tip, cause them to be subsequently distorted and rotated (Tchalenko, 1970).

Although synthetic faults are observed at mode III tips, they are not the dominant fracture type at early stages (Fig. 16A and B). As displacement increases or at a slightly lower level from the up-dip tip, synthetic faults link with extension fractures to produce pull-aparts and a zigzag fault trace (Figs. 10 and 16B; e.g. Moore and Lockner, 1995).

The en échelon fractures along mode III tips of a strike-slip fault (A in Fig. 16) are here identified as antithetic faults not extension fractures, as suggested by Scholz (1990) and by Martel and Boger (1998) (Section 3.3), for the following reasons. Firstly, tip cracks are developed at some of the fracture tips, with minor pull-aparts and displaced markers occurring rarely, indicating shear displacement (e.g. Fig. 12a and b). Secondly, the intersection angles of the fractures and master fault zone strike are typically 65° ± 10° (e.g. Figs. 3c and 12). Thirdly, most of the antithetic faults do not accumulate much displacement after synthetic faults are generated, and they are passively distorted or rotated (e.g. Figs. 10 and 12b). Fourthly, the model follows a similar evolution to those observed in the classical Riedel experiment (Riedel, 1929), and in shear box tests and earthquake fractures (Tchalenko, 1970; Tchalenko and Ambraseys, 1970).

The mode II near-tip stress concentration has a characteristic form (Lawn, 1993) that has been widely used to predict the distribution and orientation in which secondary fractures propagate (Pollard et al., 1982; Ingraffea, 1987; Pollard and Segall, 1987; Cruikshank, 1991; Reches and Lockner, 1994). Numerical models suggest the secondary fractures should nucleate toward the fault tip, where tensile stresses are highest (Kassir and Sih, 1975), and propagate beyond the fault tip (Fig. 16C and D; Cooke, 1997; Martel and Boger, 1998). Various damage zone geometries have been described at mode II tips (Fig. 16D; e.g. Chinnery, 1966b; Granier, 1985; McGrath and Davison, 1995; Martel and Boger, 1998), with antithetic faults commonly developing. Although these antithetic faults have similar angular relationship with antithetic faults at mode III tips, they tend to increase in length and spacing away from the fault tip, to form a wedge-shaped pattern (McGrath and Davison, 1995). Also, some synthetic branching faults commonly occur at mode II fault tips (Fig. 16D), forming bounding faults for block rotation. A tip crack or wing crack model with pre-existing flaws (Brace and Bombolakis, 1963; Chinnery, 1966a,b; Nemat-Nasser and Horii, 1982; Segall and Pollard, 1983; Petit and Barquins, 1988; Willemse and Pollard, 1998) is mainly applicable to mode II fault tips and segment linkage (Fig. 17). Our new 3D models can explain the variety of the damage patterns around strike-slip faults, which were not completely explained by the models of Scholz (1990) or of Martel and Boger (1998).

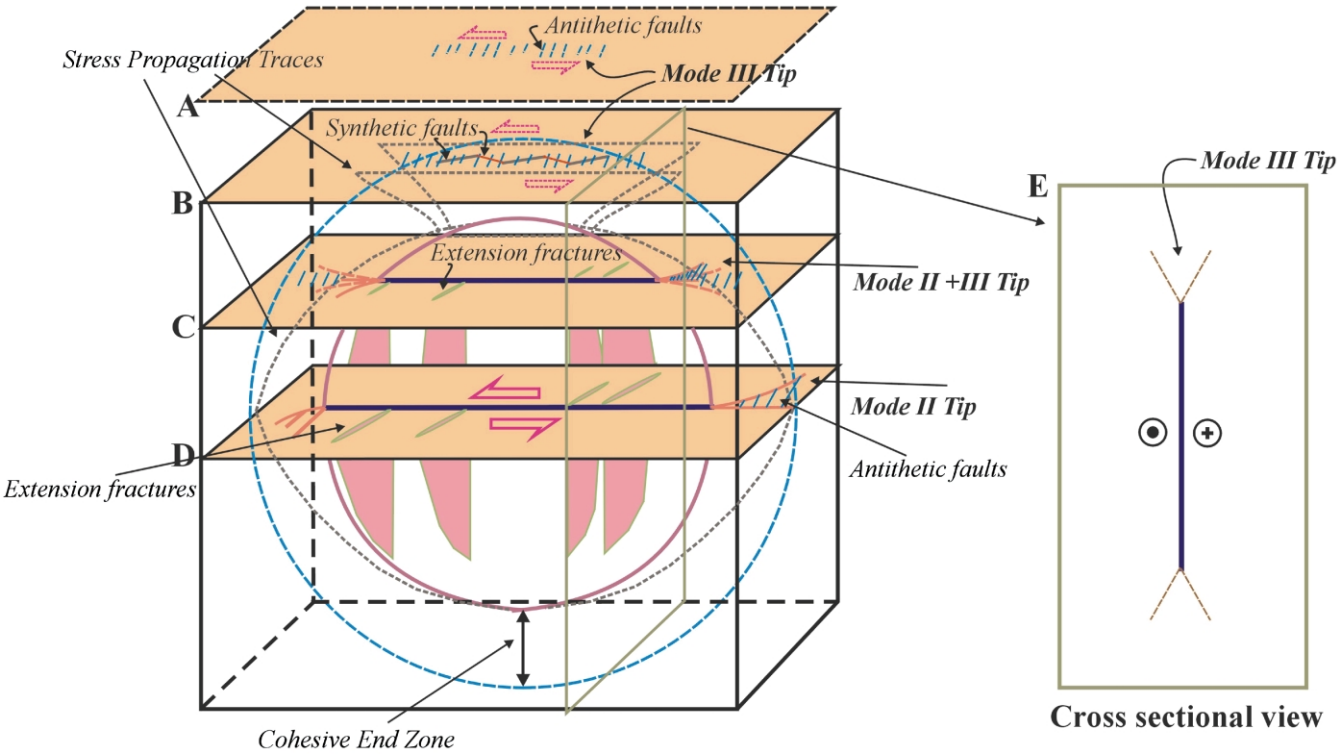

Fig. 16. Conceptual 3D model of a small displacement vertical strike-slip fault and its damage zone. The geometries of damage zones in such fault zones depend on tip modes and therefore on the location on the fault tip line.

Scholz (1990) suggested a simple 3D model for faults and secondary fractures, but did not differentiate between secondary fracture patterns at the initial stage of fault generation (Fig. 11a) and at the mode III tips of a propagating fault (Fig. 12). Martel and Boger (1998) presented a conceptual model of a penny-shaped strike-slip fault and secondary fractures. They suggested that the different fracture patterns and orientations are mainly controlled by the locations of extension fractures around a fault plane, and by stress drops during fault displacement. The Martel and Boger (1998) model does not, however, explain several phenomena in damage zones: (1) wedge-shaped antithetic faults at mode II fault tips, (2) the various patterns of synthetic and antithetic faults at mode III fault tips, (3) bifurcating fractures on cross-sections through mode III fault tips, and (4) overstepping branch faults, antithetic faults and extension fractures at mode II fault tips. Our model (Fig. 16) does account for these phenomena, with damage zone geometries depending on the slip mode and the evolution stage at each tip.

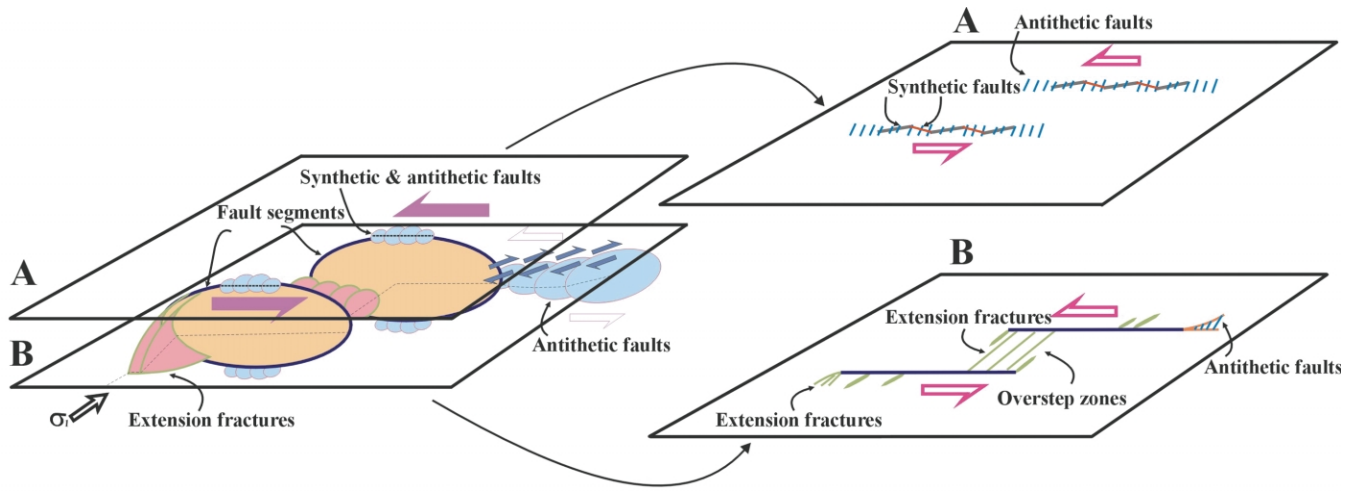

Fig. 17. A simplified conceptual 3D model for a strike-slip fault zone and linking damage zone at mode II and III fault tips. The distribution of damage zones is different at the two fault tips (A and B) showing different patterns of synthetic faults, antithetic faults and extension fractures.

8. Conclusions

1. Conjugate sets of strike-slip faults are developed in the Miocene Limestones to the west of Marsalforn, Gozo. The regional σ_1 orientation inferred from the fault data is about N070°. Most of the extension fractures that formed prior to the nucleation of the faults are sub-parallel to this orientation. Some of these pre-existing fractures were reactivated as faults, and they tend to be longer and more widely distributed than the extension fractures that developed in the local stress fields at fault tips.
2. Damage zones can be divided into three groups (distributed damage, tip damage, linking damage) based on their position along fault traces. Tip damage zones typically show antithetic faults and extension fractures in wedge-shaped damage zones at along-strike fault tips. Linking damage zones show a high intensity of faults and extension fractures in oversteps between faults (e.g. Figs. 10 and 17). Distributed damage zones are relatively long and narrow, being approximately evenly distributed along the fault strike; they tend to be dominated by antithetic faults or extension fractures.
3. The dominant geometry of damage zones at along-strike tips are wedge-shaped patterns of antithetic faults widening away from a tip, commonly accompanied by block rotation in linkage zones. At up- and down-dip tips, early-developed antithetic faults are intersected by later synthetic faults. The faults combined with extension fractures to form pull-aparts.
4. There are distinct orders in space and time of fracture development in damage zones, and in the inferred rotation of stress axes within individual fault zones. The structures developed in the damage zones have similar angular relationships to the corresponding fault through all orders.
5. Three fault growth models are proposed for the fracture patterns in damage zones observed on Gozo: (1) faults initiate as, and are dominated by, extension fractures; (2) faults propagate along-strike, with fault segments linking through tip cracks; and (3) faults propagate up- and down-dip, and show a simple fault pattern with pull-aparts. These models are dependent on the master fault tip modes as well as the location on the tip line (or evolutionary stage) of the master fault (Figs. 16 and 17).

Acknowledgements

Fieldwork for this paper was partly funded by Shell and Elf UK, which is gratefully acknowledged. We thank Barry Marsh for photographic processing. Jonathon Caine, James Evans and an anonymous reviewer are thanked for their useful suggestions, which greatly improved this paper.

References

Arboleya, M.L., Engelder, T., 1995. Concentrated slip zones with subsidiary shears: their development on three scales in the Cerro Brass Fault Zone, Appalachian Valley and Ridge. Journal of Structural Geology 17, 519–532.

Atkinson, B.K., 1987. Introduction to fracture mechanics and its geophysical applications. In: Atkinson, B.K., (Ed.), Fracture Mechanics of Rock, Academic Press Geology Series, pp. 1–26.

Bartlett, W.L., Friedman, M., Logan, J.M., 1981. Experimental folding and faulting of rocks under confining pressure. Part IX. Wrench faults in limestone layers. Tectonophysics 79, 255–277.

Bilham, R., Williams, P., 1985. Sawtooth segmentation and deformation processes on the southern San Andreas fault, California. Geophysical Research Letters 12, 557–560.

Boccaletti, M., Cello, G., Tortorici, L., 1987. Transtensional tectonics in the Sicily Channel. Journal of Structural Geology 9, 869–876.

Brace, W.F., Bombolakis, E.G., 1963. A note on brittle crack growth in compression. Journal of Geophysical Research 68, 3709–3713.

Bürgmann, R., Pollard, D.D., Martel, S.J., 1994. Slip distributions on faults: effects of stress gradients, inelastic deformation, heterogeneous host-rock stiffness, and fault interaction. Journal of Structural Geology 16, 1675–1690.

Caine, J.S., Forster, C.B., 1999. Fault zone architecture and fluid flow: insights from field data and numerical modeling. In: Haneberg, W.C., Mozley, P.S., Moore, J.C., Goodwin, L.B. (Eds.), Faults and Sub-Surface Fluid Flow in the Shallow Crust. American Geophysical Union Monograph 113, pp. 101–127.

Caine, J.S., Evans, J.P., Forster, C.B., 1996. Fault zone architecture and permeability structure. Geology 24, 1025–1028.

Cartwright, J.A., Trudgill, B.D., Mansfield, C.S., 1995. Fault growth by segment linkage: an explanation for scatter in maximum displacement and trace length data from the Canyonlands Grabens of SE Utah. Journal of Structural Geology 17, 1319–1326.

Chester, F.M., Logan, J.M., 1986. Implications for mechanical properties of brittle faults from observations of the Punchbowl fault zone, California. Pure and Applied Geophysics 124, 79–106.

Chinnery, M.A., 1966a. Secondary faulting: I. Theoretical aspects. Canadian Journal of Earth Sciences 3, 163–174.

Chinnery, M.A., 1966b. Secondary faulting: II. Geological aspects. Canadian Journal of Earth Sciences 3, 175–190.

Christie-Blick, N., Biddle, K.T., 1985. Deformation and basin formation along strike-slip faults. In: Biddle, K.T., Christie-Blick, N. (Eds.), Strike-slip Deformation, Basin Formation, and Sedimentation. Society of Economic Palaeontologists and Mineralogists. Special Publication 37, pp. 1–34.

Connolly, P., Cosgrove, J., 1999. Prediction of fracture-induced permeability and fluid flow in the crust using experimental stress data. Bulletin of the American Association of Petroleum Geologists 83, 757–777.

Cooke, M.L., 1997. Fracture localization along faults with spatially varying friction. Journal of Geophysical Research 102, 22425–22434.

Cowie, P.A., Scholz, C.H., 1992. Physical explanation for the displacement-length relationship for faults using a post-yield fracture mechanics model. Journal of Structural Geology 14, 1133–1148.

Cowie, P.A., Shipton, Z.K., 1998. Fault tip displacement gradients and process zone dimensions. Journal of Structural Geology 20, 983–997.

Cox, S.J.D., Scholz, C.H., 1988. On the formation and growth of faults: an experimental study. Journal of Structural Geology 10, 413–430.

Crider, J.G., Pollard, D.D., 1998. Fault linkages: three-dimensional mechanical interaction between échelon normal faults. Journal of Geophysical Research 103, 24373–24391.

Crowell, J.C., 1974. Origin of late Cenozoic basins in southern California. In: Dickinson, W.R. (Ed.), Tectonics and Sedimentation. Society of Economic Paleontologists and Mineralogists Special Publication 22, pp. 190–204.

Cruikshank, K.M., 1991. Analysis of minor fractures associated with joints and faulted joints. Journal of Structural Geology 13, 865–886.

Davis, G.H., Bump, A.B., Garcia, P.E., Ahlgren, S.G., 2000. Conjugate Riedel deformation band shear zones. Journal of Structural Geology 22, 169–190.

Debono, G., Xerri, S., 1993. Geological map of the Maltese islands. Sheet 2, Gozo and Comino, 1:25,000.

Dholakia, S.K., Aydin, A., Pollard, D.D., Zoback, M.D., 1998. Fault-controlled hydrocarbon pathways in the Monterey formation, California. Bulletin of the American Association of Petroleum Geologists 82, 1551–1574.

Finetti, I., 1984. Geophysical study of the Sicily Channel rift zone. Bollettino di Geofisica Teorica e Applicata 26, 3–28.

Fletcher, R.C., Pollard, D.D., 1981. Anti-crack model for pressure solution surfaces. Geology 9, 419–424.

Gamond, J.F., 1983. Displacement features associated with fault zones: a comparison between observed examples and experimental models. Journal of Structural Geology 5, 33–45.

Gamond, J.F., 1987. Bridge structures as sense of displacement criteria in brittle fault zones. Journal of Structural Geology 9, 609–620.

Granier, T., 1985. Origin, damping and pattern of development of faults in granite. Tectonics 4, 721–737.

Gupta, A., Scholz, C., 2000. A model of normal fault interaction based on observations and theory. Journal of Structural Geology 22, 865–879.

Hancock, P.L., 1985. Brittle microtectonics: principles and practice. Journal of Structural Geology 7, 437–457.

Harding, T.P., Vierbuchen, R.C., Christie-Blick, N., 1985. Structural styles, plate-tectonic settings, and hydrocarbon traps of divergent (transtensional) wrench faults. In: Biddle, K.T., Christie-Blick, N. (Eds.), Strike-slip Deformation, Basin Formation, and Sedimentation. Society of Economic Palaeontologists and Mineralogists. Special Publication 37, pp. 51–77.

Horii, H., Nemat-Nasser, S., 1985. Compressive-induced microcrack growth in brittle solids: axial splitting and shear failure. Journal of Geophysical Research 90, 3105–3125.

Ingraffea, A.D., 1987. Theory of crack initiation and propagation in rock. In: Atkinson, B.K., (Ed.), Fracture Mechanics of Rocks, Academic Press, San Diego, California, pp. 71–108.

Kassir, M.K., Sih, G.C., 1975. Three-Dimensional Crack Problems, Noordhoof, Leiden, Netherlands, 452pp.

Kim, Y.S., Andrews, J.R., Sanderson, D.J., 2000. Damage zones around strike-slip fault systems and strike-slip fault evolution, Crackington Haven, southwest England. Geoscience Journal 4, 53–72.

Kim, Y.S., Andrews, J.R., Sanderson, D.J., 2001. Reactivated strike-slip faults: examples from north Cornwall, UK. Tectonophysics 340, 173–194.

Lawn, B., 1993. Fracture of Brittle Solids, 2nd ed, Cambridge University Press, New York, 378pp.

Long, J.C.S., Witherspoon, P.A., 1985. The relationship of the degree of interconnection to permeability in fracture networks. Journal of Geophysical Research 90, 3087–3098.

Mandl, G., 1988. The mechanics of tectonic faulting; models and basic concepts. In: Zwart, H.J. (Ed.), Developments in Structural Geology. Elsevier, Amsterdam, 408pp.

Martel, S.J., 1990. Formation of compound strike-slip fault zones, Mount Abbot quadrangle, California. Journal of Structural Geology 12, 869–882.

Martel, S.J., 1997. Effects of cohesive zones on small faults and implications for secondary fracturing and fault trace geometry. Journal of Structural Geology 19, 835–847.

Martel, S.J., Boger, W.A., 1998. Geometry and mechanics of secondary fracturing around small three-dimensional faults in granitic rock. Journal of Geophysical Research 103, 21299–21314.

Martel, S.J., Pollard, D.D., Segall, P., 1988. Development of simple fault zones in granitic rock, Mount Abbot quadrangle, Sierra Nevada, California. Bulletin of the Geological Society of America 100, 1451–1465.

McGrath, A.G., Davison, I., 1995. Damage zone geometry around fault tips. Journal of Structural Geology 17, 1011–1024.

McKinstry, H.E., 1953. Shears of the second order. American Journal of Science 251, 401–414.

Mollema, P.N., Antonellini, M., 1999. Development of strike-slip faults in the dolomites of the Sella Group, Northern Italy. Journal of Structural Geology 21, 273–292.

Moody, J.D., Hill, M.J., 1956. Wrench-fault tectonics. Bulletin of the Geological Society of America 67, 1207–1246.

Moore, D.E., Lockner, D.A., 1995. The role of microcracking in shear-fracture propagation in granite. Journal of Structural Geology 17, 95–114.

Morgenstern, N.R., Tchalenko, J.S., 1967. Microscopic structures in kaolin subjected to direct shear. Geotechnique 17, 309–328.

National Academy of Science, 1996. Rock Fractures and Fluid Flow: Contemporary Understanding and Application, National Research Council, Washington, DC.

Naylor, M.A., Mandl, G., Sijpesteijn, C.H.K., 1986. Fault geometries in basement-induced wrench faulting under different initial stress states. Journal of Structural Geology 8, 737–752.

Nemat-Nasser, S., Horii, H., 1982. Compression-induced nonplanar crack extension with application to splitting, exfoliation, and rockburst. Journal of Geophysical Research 87, 6805–6821.

Peacock, D.C.P., 1991. Displacements and segment linkage in strike-slip fault zones. Journal of Structural Geology 13, 1025–1035.

Peacock, D.C.P., 2001. The temporal relationship between joints and faults. Journal of Structural Geology 23, 329–341.

Peacock, D.C.P., Sanderson, D.J., 1995a. Strike-slip relay ramps. Journal of Structural Geology 17, 1351–1360.

Peacock, D.C.P., Sanderson, D.J., 1995b. Pull-aparts, shear fractures and pressure solution. Tectonophysics 241, 1–13.

Pedley, H.M., House, M.R., Waugh, B., 1976. The Geology of Malta and Gozo. Proceedings of the Geologists Association 87, 325–341.

Petit, J.P., Barquins, M., 1988. Can natural faults propagate under Mode II conditions? Tectonics 7, 1243–1256.

Petit, J.P., Mattauer, M., 1995. Paleostress superimposition deduced from mesoscale structures in limestone: the Matelles exposure, Languedoc, France. Journal of Structural Geology 17, 245–256.

Pollard, D.D., Segall, P., 1987. Theoretical displacements and stresses near fractures in rock: with applications to faults, joints, veins, dikes, and solution surfaces. In: Atkinson, B.K., (Ed.), Fracture Mechanics of Rock, Academic Press Geology Series, Academic Press, pp. 277–349.

Pollard, D.D., Segall, P., Delaney, P.T., 1982. Formation and interpretation of dilatant échelon cracks. Bulletin Geological Society of America 93, 1291–1303.

Reches, Z., Lockner, D.A., 1994. Nucleation and growth of faults in brittle rocks. Journal of Geophysical Research 99, 18159–18173.

Riedel, W., 1929. Zur Mechanik geologischer Brucherscheinungen. Zentrablatt für Mineralogie, Geologie, und Palaeontologie 1929B, 354–368.

Rispoli, R., 1981. Stress fields about strike-slip faults inferred from stylolites and tension gashes. Tectonophysics 75, T29–T36.

Rodgers, D.A., 1980. Analysis of pull-apart basin development produced by en échelon strike-slip faults, In: Balance, P.F., Reading, H.G. (Eds.), Sedimentation at Oblique-Slip Margins. International Association of Sedimentologists, Special Publication 4, pp. 27–41.

Scholz, C.H., 1968. Microfractures, aftershocks, and seismicity. Seismological Society of America Bulletin 58, 1117–1130.

Scholz, C.H., 1990. The Mechanics of Earthquakes and Faulting, Cambridge University Press, Cambridge, 439pp.

Schreurs, G., 1994. Experiments on strike-slip faulting and block rotation. Geology 22, 567–570.

Segall, P., Pollard, D.D., 1980. Mechanics of discontinuous faults. Journal of Geophysical Research 85, 4337–4350.

Segall, P., Pollard, D.D., 1983. Nucleation and growth of strike slip faults in granite. Journal of Geophysical Research 88, 555–568.

Sibson, R.H., 1996. Structural permeability of fluid-driven fault-fracture meshes. Journal of Structural Geology 18, 1031–1042.

Sims, D., Ferrill, D.A., Stamatakos, J.A., 1999. Role of a ductile decollement in the development of pull-apart basins: experimental results and natural examples. Journal of Structural Geology 21, 533–554.

Swanson, M.T., 1988. Pseudotachylyte-bearing strike-slip duplex structures in the Fort Foster Brittle Zone, Southern Maine. Journal of Structural Geology 10, 813–828.

Sylvester, A.G., 1988. Strike-slip faults. Bulletin of the Geological Society of America 100, 1666–1703.

Sylvester, A.G., Smith, R.R., 1976. Tectonic transpression and basement-controlled deformation in San Andreas fault zone, Salton Trough, California. Bulletin of the American Association of Petroleum Geologists 60, 2018–2102.

Tchalenko, J.S., 1970. Similarities between shear zones of different magnitudes. Bulletin of the Geological Society of America 81, 1625–1640.

Tchalenko, J.S., Ambraseys, N.N., 1970. Structural analysis of the Dasht-e Bayaz (Iran) earthquake fractures. Bulletin of the Geological Society of America 81, 41–60.

Vermilye, J.M., Scholz, C.H., 1999. Fault propagation and segmentation: insight from the microstructural examination of a small fault. Journal of Structural Geology 21, 1623–1636.

Wilcox, R.E., Harding, T.P., Seely, D.R., 1973. Basic wrench tectonics. Bulletin of the American Association of Petroleum Geologists 57, 74–96.

Willemse, E.J.M., Peacock, D.C.P., Aydin, A., 1997. Nucleation and growth of strike-slip faults in limestones from Somerset, UK. Journal of Structural Geology 19, 1461–1477.

Willemse, E.J.M., Pollard, D.D., 1998. On the orientation and patterns of wing cracks and solution surfaces at the tips of a sliding flaw or fault. Journal of Geophysical Research 103, 2427–2438.

Wu, S., Groshong, R.H., 1991. Low-temperature deformation of sandstone, southern Appalachian fold-thrust belt. Bulletin of the Geological Society of America 103, 861–875.